INFORMATION TO USERS

This material was produced from a microfilm copy of the original document. While the most advanced technological means to photograph and reproduce this document have been used, the quality is heavily dependent upon the quality of the original submitted.

The following explanation of techniques is provided to help you understand markings or patterns which may appear on this reproduction.

1. The sign or "target" for pages apparently lacking from the document photographed is "Missing Page(s)". If it was possible to obtain the missing page(s) or section, they are spliced into the film along with adjacent pages. This may have necessitated cutting thru an image and duplicating adjacent pages to insure you complete continuity.

2. When an image on the film is obliterated with a large round black mark, it is an indication that the photographer suspected that the copy may have moved during exposure and thus cause a blurred image. You will find a good image of the page in the adjacent frame.

3. When a map, drawing or chart, etc., was part of the material being photographed the photographer followed a definite method in "sectioning" the material. It is customary to begin photoing at the upper left hand corner of a large sheet and to continue photoing from left to right in equal sections with a small overlap. If necessary, sectioning is continued again — beginning below the first row and continuing on until complete.

4. The majority of users indicate that the textual content is of greatest value, however, a somewhat higher quality reproduction could be made from "photographs" if essential to the understanding of the dissertation. Silver prints of "photographs" may be ordered at additional charge by writing the Order Department, giving the catalog number, title, author and specific pages you wish reproduced.

5. PLEASE NOTE: Some pages may have indistinct print. Filmed as received.

Xerox University Microfilms
300 North Zeeb Road
Ann Arbor, Michigan 48106

Downloaded from SHAREOK. Persistent Handle URL: https://hdl.handle.net/11244/3859

75-6539

MORELAND, Richard Foster, 1937-
THERMOELECTRIC SIZE EFFECT IN NOBLE METALS.

The University of Oklahoma, Ph.D., 1974
Physics, solid state

Xerox University Microfilms, Ann Arbor, Michigan 48106

THIS DISSERTATION HAS BEEN MICROFILMED EXACTLY AS RECEIVED.

THE UNIVERSITY OF OKLAHOMA

GRADUATE COLLEGE

THERMOELECTRIC SIZE EFFECT IN NOBLE METALS

A DISSERTATION

SUBMITTED TO THE GRADUATE FACULTY

in partial fulfillment of the requirements for the

degree of

DOCTOR OF PHILOSOPHY

By

RICHARD FOSTER MORELAND

Norman, Oklahoma

1974

THERMOELECTRIC SIZE EFFECT IN NOBLE METALS

APPROVED BY

Ronald R. Bowrassa

B. Foote

David Branch

Dennis Shaw

Gerald Tuma

DISSERTATION COMMITTEE

ACKNOWLEDGMENTS

This work is dedicated to my wife, Julie, and daughter, Lisa, whose sacrifice made this dissertation possible.

This research program was funded by the United States Atomic Energy Commission under Contract AT-(40-1)-3940.

A grant from the Research Corporation made preliminary work on this project possible.

TABLE OF CONTENTS

ACKNOWLEDGMENTS iii

LIST OF TABLES. vi

LIST OF ILLUSTRATIONS vii

Chapter

I. INTRODUCTION. 1

Size Effect on the Electronic Component of the Thermoelectric Power at High Temperatures. 1

The Effect of Magnetic Impurities on the Thermoelectric Power at Low Temperatures 5

Other Possible Low-Temperature Thermoelectric Effects . 6

Dugdale and Bailyn Theory of Phonon-Drag 9

Nielson-Taylor Theory of Diffusion Thermoelectric Power 9

This Experiment 10

II. THEORY. 11

High Temperature Thermoelectric Size Effect 11

Low Temperature Thermoelectric Size Effect. 14

Effect of Iron Impurities. 14

Change in the Phonon-Drag Thermoelectric Power . . 17

Change in the Electronic Thermoelectric Power. . . 23

III. THE EXPERIMENT. 25

Sample Preparation. 25

Annealing Techniques. 27

Sample Holder 28

Thermoelectric Emf Measurements 28

Resistance Measurement. 29

Temperature Measurement 29

Experimental Procedure. 33

TABLE OF CONTENTS (Cont'd.)

Chapter		Page
IV.	RESULTS AND ANALYSIS.	36
	Thermoelectric Power Curves for Gold, Copper, and Silver	36
	Analysis of High Temperature Results.	55
	Analysis of Low Temperature Results	63
	Method I	64
	Method II.	66
V.	DISCUSSION AND CONCLUSIONS.	72
	High Temperature Results.	72
	Low Temperature Results	74
	Sources of Error.	76
LIST OF REFERENCES.		77

LIST OF TABLES

Table		Page
1.	High Temperature Results $\{\frac{\partial \ell n \ell(\varepsilon)}{\partial \ell n \varepsilon}\}_{\varepsilon_F}$, $\{\frac{\partial \ell n A(\varepsilon)}{\partial \ell n \varepsilon}\}_{\varepsilon_F}$ . . .	62
2.	Values of Low Temperature Fitting Parameter $\rho_3 S_o$ . . .	65
3.	Method I: Values of Iron Resistivity and Concentration	67
4.	Method II: Values of Parameters for Gold	69
5.	Method II: Values of Parameters for Copper	70
6.	Method II: Values of Parameters for Silver	71

LIST OF ILLUSTRATIONS

Figure — Page

1. Sample holder and sample 26

2. (a) Thermoelectric emf measurement 30
   (b) Resistance measurement 30

3. Schematic diagram of controller with modifications . . 32

4. Perspective view indicating method of sample transfer from annealing block to sample holder 34

5. Sample Au 1. Difference ΔS between the thermoelectric power of a gold foil of thickness $a_1 = 2.54 \times 10^{-2}$ mm and a gold wire of diameter $a_2 = 0.254$ mm as a function of temperature. ($RR_{wire} = 1328$ and $RR_{foil} = 442$) 37

6. Sample Au 2. Difference ΔS between the thermoelectric power of a gold foil to thickness $a_1 = 1.27 \times 10^{-2}$ mm and a gold wire of diameter $a_2 = 0.254$ mm as a function of temperature. ($RR_{wire} = 1074$ and $RR_{foil} = 199$) 38

7. Sample Au 3. Difference ΔS between the thermoelectric power of a gold foil of thickness $a_1 = 5.08 \times 10^{-3}$ mm and a gold wire of diameter $a_2 = 0.254$ mm as a function of temperature. ($RR_{wire} = 1081$ and $RR_{foil} = 136$) 39

8. Sample Au 4. Difference ΔS between the thermoelectric power of a gold foil of thickness $a_1 = 2.54 \times 10^{-3}$ mm and a gold wire of diameter $a_2 = 0.254$ mm as a function of temperature. ($RR_{wire} = 1329$ and $RR_{foil} = 96$)..... 40

9. Sample Au 5. Difference ΔS between the thermoelectric power of a gold foil of thickness $a_1 = 2.03 \times 10^{-3}$ mm and a gold wire of diameter $a_2 = 0.254$ mm as a function of temperature. ($RR_{wire} = 1441$ and $RR_{foil} = 100$)

10. Sample Au 6. Difference ΔS between the thermoelectric power of a gold foil of thickness $a_1 = 1.52 \times 10^{-3}$

LIST OF ILLUSTRATIONS (Cont'd.)

Figure — Page

mm and a gold wire of diameter a_2 = 0.254 mm as a function of temperature. (RR_{wire} = 1683 and RR_{foil} = 77). 42

11. Sample Cu 1. Difference ΔS between the thermoelectric power of a copper foil of thickness $a_1 = 2.54 \times 10^{-2}$ mm and a copper wire of diameter a_2 = 0.254 mm as a function of temperature. (RR_{wire} = 1441 and RR_{foil} = 558) 43

12. Sample Cu 2. Difference ΔS between the thermoelectric power of a copper foil of thickness $a_1 = 1.27 \times 10^{-2}$ mm and a copper wire of diameter a_2 = 0.254 mm as a function of temperature. (RR_{wire} = 1244 and RR_{foil} = 243) 44

13. Sample Cu 3. Difference ΔS between the thermoelectric power of a copper foil of thickness $a_1 = 5.08 \times 10^{-3}$ mm and a copper wire of diameter a_2 = 0.254 mm as a function of temperature. (RR_{wire} = 1538 and RR_{foil} = 91). 45

14. Sample Cu 4. Difference ΔS between the thermoelectric power of a copper foil of thickness $a_1 = 2.54 \times 10^{-3}$ mm and a copper wire of diameter a_2 = 0.254 mm as a function of temperature. (RR_{wire} = 1307 and RR_{foil} = 102) 46

15. Sample Cu 5. Difference ΔS between the thermoelectric power of a copper foil of thickness $a_1 = 2.03 \times 10^{-3}$ mm and a copper wire of diameter a_2 = 0.254 mm as a function of temperature. (RR_{wire} = 1158 and RR_{foil} = 90). 47

16. Sample Cu 6. Difference ΔS between the thermoelectric power of a copper foil of thickness $a_1 = 1.52 \times 10^{-3}$ mm and a copper wire of diameter a_2 = 0.254 mm as a function of temperature. (RR_{wire} = 1379 and RR_{foil} = 69). 48

17. Sample Ag 1. Difference ΔS between the thermoelectric power of a silver foil of thickness $a_1 = 2.54 \times 10^{-2}$ mm and a silver wire of diameter a_2 = 0.254 mm as a function of temperature. (RR_{wire} = 1500 and RR_{foil} = 450) 49

LIST OF ILLUSTRATIONS (Cont'd.)

Figure Page

18. Sample Ag 2. Difference ΔS between the thermoelectric power of a silver foil of thickness $a_1 = 1.27 \times 10^{-2}$ mm and a silver wire of diameter $a_2 = 0.254$ mm as a function of temperature. ($RR_{wire} = 1472$ and $RR_{foil} = 266$) 50

19. Sample Ag 3. Difference ΔS between the thermoelectric power of a silver foil of thickness $a_1 = 5.08 \times 10^{-3}$ mm and a silver wire of diameter $a_2 = 0.254$ mm as a function of temperature. ($RR_{wire} = 1525$ and $RR_{foil} = 158$) 51

20. Sample Ag 4. Difference ΔS between the thermoelectric power of a silver foil of thickness $a_1 = 2.54 \times 10^{-3}$ mm and a silver wire of diameter $a_2 = 0.254$ mm as a function of temperature. ($RR_{wire} = 1410$ and $RR_{foil} = 96$)..... 52

21. Sample Ag 5. Difference ΔS between the thermoelectric power of a silver foil of thickness $a_1 = 2.03 \times 10^{-3}$ mm and a silver wire of diameter $a_2 = 0.254$ mm as a function of temperature. ($RR_{wire} = 1580$ and $RR_{foil} = 90$). 53

22. Sample Ag 6. Difference ΔS between the thermoelectric power of a silver foil of thickness $a_1 = 1.52 \times 10^{-3}$ mm and a silver wire of diameter $a_2 = 0.254$ mm as a function of temperature. ($RR_{wire} = 1726$ and $RR_{foil} = 61$). 54

23. Difference between the electrical resistivity of a gold foil of thickness a_1 and a gold wire of diameter $a_2 = 0.254$ mm, calculated from Eq. (53) for $T' = 77.3\ ^{o}K$ (circles) and $T' = 4.2\ ^{o}K$ (squares). 56

24. Difference between the electrical resistivity of a copper foil of thickness a_1 and a copper wire of diameter $a_2 = 0.254$ mm, calculated from Eq. (53) for $T' = 77.3\ ^{o}K$ (circles) and $T' = 4.2\ ^{o}K$ (squares). 58

25. Difference between the electrical resistivity of a silver foil of thickness a_1 and a silver wire of diameter $a_2 = 0.254$ mm, calculated from Eq.

LIST OF ILLUSTRATIONS (Cont'd.)

Figure		Page
	(53) for T' = 77.3 °K (circles) and T' = 4.2 °K (squares).	59
26.	Difference between the thermoelectric power of a foil of thickness a_1 and a wire of diameter a_2 = 0.254 mm in the temperature range between 100 and 296 °K for gold and silver and between 250 and 296 °K for copper.	61

CHAPTER I

INTRODUCTION

It is observed experimentally that when a metal is subjected to a temperature gradient there arises within the material an electric field. This field is proportional to the magnitude of the temperature gradient, and the constant of proportionality is known as the absolute thermoelectric power, or thermopower, of the metal.

The absolute thermoelectric power, S^o, of a pure metal consists of a contribution, S_e^o, arising from the non-equilibrium distribution of the conduction electrons, and a contribution, S_g^o, caused by the interaction of the conduction electrons and the phonons, which are not in equilibrium:

$$S^o = S_e^o + S_g^o \quad . \tag{1}$$

S_e^o and S_g^o are called the electronic (or diffusion) thermoelectric power and the phonon-drag thermoelectric power, respectively.

Size Effect on the Electronic Component of the Thermoelectric Power at High Temperatures

The electronic thermoelectric power of a pure metal can be written as[1]

$$S_e^o = \frac{\pi^2 k_B^2 T}{3e\epsilon_F} \left\{\frac{\partial \ell n \sigma(\epsilon)}{\partial \ell n \epsilon}\right\}_{\epsilon_F} \quad , \tag{2}$$

where e is the charge of the major carrier, ε is the energy of the conduction electrons, ε_F is the Fermi energy, k_B is Boltzman's constant, T is the absolute temperature, and σ is the electrical conductivity of the conduction electrons considered as a function of electron energy. A simple expression for the electrical conductivity[2] is

$$\sigma(\varepsilon)\alpha v^2(\varepsilon)\tau(\varepsilon)N(\varepsilon) \ , \tag{3}$$

where v is the average velocity of the conduction electrons, τ the relaxation time, and N the density of electron states. In a free-electron picture, $v^2\alpha\varepsilon$, $\tau\alpha\varepsilon^{3/2}$, and $N\alpha\varepsilon^{1/2}$.[3] Thus, the free-electron theory predicts

$$\left\{ \frac{\partial \ell n\sigma(\varepsilon)}{\partial \ell n\varepsilon} \right\}_{\varepsilon_F} = 3 \tag{4}$$

and S_e^o is negative if the carriers are electrons as determined by the Hall effect.

The positive sign of the electronic thermoelectric power of the noble metals has been a nagging embarrassment to the theory of ordinary electron transport properties of solids for a number of years.

Equation (2) can also be written as,[3]

$$S_e^o = \frac{\pi^2 k_B^2 T}{3e\varepsilon_F} \{U+V\}_{\varepsilon_F} \ . \tag{5}$$

The parameters U and V are given by

$$U = \frac{\partial \ell n\ell(\varepsilon)}{\partial \ell n\varepsilon} \quad \text{and} \quad V = \frac{\partial \ell nA(\varepsilon)}{\partial \ell n\varepsilon} \ , \tag{6}$$

where ℓ is the mean free path of the conduction electrons, and A is the area of a constant energy surface. In order for the electronic thermoelectric power to be positive the bracket in Eq. (5) must be negative, or the major carriers must be holes.

When it was found that the Fermi surface in the noble metals is distorted and touches the zone boundary, it was suggested[4] that the area of the Fermi surface, A, might decrease sufficiently fast with increasing energy to make V negative. From an analysis of the transport properties of the noble metals Ziman[5], in 1961, concluded that V is reduced below the free-electron value of 1, but still remains positive. He estimated V to be in the range between 0 and 0.5. It would then follow that the positive sign of S_e^o must have its origin in the first term in the brackets of Eq. (5).

Ziman[5] argued that in the noble metals the electron mean free path should be anistropic over the Fermi surface, and that a more complete theory of the function $\ell(\varepsilon)$ was necessary to explain the positive electronic thermoelectric power. Unfortunately, a detailed calculation by Taylor[6] in 1963 once more yielded a negative electronic thermoelectric power for copper.

In 1964, Blatt[7] proposed a mechanism based on electron-electron scattering which could lead to an $\ell(\varepsilon)$ which displays the characteristics necessary for a positive electronic thermoelectric power. Later work[8] indicated that this effect was not appreciable in the noble metals.

In 1967, Robinson[9] demonstrated in a model calculation that the electronic thermoelectric power in the noble metals can be

reasonably understood within a nearly-free-electron model if the electron-ion interaction is treated properly. He accomplishes this by using a point-ion pseudopotential to represent the electron-ion interaction. This will be explained in more detail in Chapter II, but his conclusion is that U can be in fact negative.

These theoretical attempts to discover which term is causing the sign anomaly in the noble metals have been accompanied by experimental efforts to measure U and V separately. The most successful of which is perhaps that of Heubener[10]. He has shown that U can be experimentally determined by measuring the influence of sample size on the electronic thermoelectric power. In fact, as will be shown in Chapter II,

$$\Delta S_e = S_e^{foil} - S_e^{wire} = \left(\frac{1}{2a_1} - \frac{1}{a_2}\right) \frac{\pi^2 k_B^2 T}{4e\epsilon_F} \left\{\frac{\partial \ell n \ell(\epsilon)}{\partial \ell n \epsilon}\right\}_{\epsilon_F}, \qquad (7)$$

where a_1 is the thickness of the foil and a_2 is the diameter of the wire. As can be seen from Eq. (7), thermoelectric measurements carried out with a thermocouple consisting of a thin foil and a relatively thin wire, of the same material, will yield information on the quantity U. Subsequently, V may be determined with the aid of Eq. (5) and the known value of S_e^o/T at high temperatures.

The thermoelectric size effect has been investigated in the past by numerous authors[10-24] in a series of metals. The first experiments of this kind were performed with thin-film samples prepared by evaporation[11-17]. Later experiments were carried out with thin foil samples obtained by cold rolling and subsequent annealing[10,18,21]. Recently, further experiments have been carried

out with evaporated films of the noble metals[19,20,22-24]. In the case of the noble metals the experimental results on the quantity U seem to be somewhat unclear. For gold (Au), between 77 °K and room temperature, Huebener[10] obtained a value for U of -0.53 ± 0.19. This is in agreement with the value of -0.61 ± 0.20 reported by Worobey *et al.*[24], and the value -0.60 ± 0.04 measured by Lin and Leonard[23]. These are in disagreement with the work of Angus and Dalgliesh[22], who reported a value of +0.9 in Au near room temperature. They also found values for U of +2.3 and +2.7 for copper (Cu) and silver (Ag) respectively. Gouault[19] found in Cu the value +2.1. These positive values for U in the noble metals are in disagreement with the physical picture and model calculation of Robinson[9].

In the early experiments with thin films[11-17], the work of Angus and Dalgliesh[22] and the work of Gouault[19], Lin and Leonard[23] has suggested that the value of U was disturbed because the thin films could not anneal at sufficiently high temperatures after deposition. Thus the thermoelectric size effect was probably masked by the presence of large concentrations of lattice defects within the films.

The Effect of Magnetic Impurities on the Thermoelectric Power at Low Temperatures

"Pure" samples of the noble metals, i.e. the best material available from commercial sources, exhibit an anomolous thermoelectric power at temperatures less than 20 °K due to the presence of magnetic transition metal impurities, chiefly iron[26-31]. In

1964, Kondo[32,33] investigated the scattering of conduction electrons from a magnetic impurity--and found that the results qualitatively explain the resistance minimum and anomalous thermoelectric powers observed in the noble metals. He found that at high temperatures the contribution to the thermoelectric power due to the magnetic impurity is constant, while at low temperatures it is proportional to the temperature. He suggested an interpolation formula connecting the two limits.[34]

$$S_{Fe} = S_o \frac{T}{T+T_o} \quad . \tag{11}$$

Guénault[30] has found that this formula fits the experimental results in the noble metals very well.

Other Possible Low Temperature Thermoelectric Effects

We will now introduce three other low temperature thermoelectric effects. These are neglected in the final analysis since they are all small.

Size Effect on the Phonon-Drag Component of the Thermoelectric Power.

As of yet we have not considered the effects in the electron system which are caused by the deviation of the phonon system from its equilibrium distribution. Let us imagine a stream of phonons which interacts with the conduction electrons. This is a quite familiar situation when we recall that the collisions of electrons with phonons lead directly to the electrical resistance of a conductor dependent on temperature. The phonon current present in a temperature gradient interacts with the conduction electrons and

"drags" the electrons along. Thus the term "phonon-drag."

An estimate of the phonon-drag thermoelectric power, S_g^o, can be given by[25]

$$S_g^o \simeq \frac{C_q}{Ne} \alpha \ , \tag{12}$$

where C_q is the lattice specific heat, and N the density of electron states. The parameter α is a measure of the relative probability of a phonon-electron interaction as compared with all other phonon interactions.

$$\alpha = \frac{1/\tau_{pe}}{1/\tau_{pe} + \sum_i 1/\tau_{pi}} \ , \tag{13}$$

where τ_{pe} is the relaxation time for phonon-electron interactions, and τ_{pi} is the relaxation time for each other individual phonon interaction. Thus the inclusion of additional phonon interactions should reduce the magnitude of the phonon-drag thermoelectric power as given by Eq. (12).

The phonon scattering at the crystal surface causes a change in the phonon-drag component of the thermoelectric power. Studies of the size effect on the phonon-drag thermoelectric power should yield information on the average phonon mean free path in the bulk material as a function of temperature.

The boundary scattering of phonons is analogous to the boundary scattering of electrons. Therefore, the theory developed for electrons[35] can be used directly to describe the boundary scattering of phonons. Huebener[18] has found that the change in the phonon-drag thermoelectric power between a foil of thickness a_1 and a

cylindrical wire of diameter a_2 can be expressed approximately as

$$\Delta S_g = S_g^{foil} - S_g^{wire} = -\frac{3}{4}\left(\frac{1}{2a_1} - \frac{1}{a_2}\right) S_g^o \lambda_o , \qquad (14)$$

where S_g^o is the phonon-drag thermoelectric power of the bulk material, and λ_o is the bulk mean free path of the phonons. We would expect S_g^{foil} to be smaller than S_g^{wire} due to the additional scattering of phonons at the specimen surface. Thus, we would expect Eq. (14) to predict a decrease in the change in the phonon-drag thermoelectric power between a foil and a wire.

The size effect on the phonon-drag thermoelectric power has been experimentally investigated in platinum.[18] The experiment resulted in determining the phonon mean free path as a function of temperature. Worobey *et al.*[24] have observed a reduction in the change in the phonon-drag thermoelectric power between Au films of different thickness.

An estimate of the phonon-drag size effect in the noble metals based on the analysis of Huebener gives a value of the order of 0.01 $\mu V/^oK$ (see Chapter II). This is far smaller than the effect seen in this experiment.

If, however, the thermoelectric power is enhanced at low temperatures, as is found in this experiment we must seek an explanation other than ordinary phonon-drag size effect. Two possible explanations have been advanced, and are described in the following paragraphs.

Dugdale and Bailyn Theory of Phonon-Drag.

One explanation was suggested by Dugdale and Bailyn[36] and is based on the fact that the Fermi surface in most metals is far from a simple sphere. The contribution to S_g^o from the various parts of the Fermi surface vary greatly in both sign and magnitude. This idea will be discussed in more detail in Chapter II, but the theory can not yet be applied to the case of surface scattering. That must await measurement of the anisotropy of surface scattering over the Fermi surface. Techniques have been developed recently to measure anisotropy of impurity and phonon scattering, but as yet there is no method to study the anisotropy of surface scattering.

Nielson-Taylor Theory of Diffusion Thermoelectric Power.

Another explanation is to look at the work of Nielson and Taylor[37-39] on the theory of thermoelectric effects in metals and alloys. They have applied second-order corrections to the T-matrix for electron scattering involving intermediate phonon states. Their results give an additional contribution to the electronic thermoelectric power of a metal or alloy which has the same magnitude and general temperature dependence as that attributed to phonon-drag. The sign of the effect is determined by the details of the scattering potential that the electrons see. This has met with some success in explaining anomolous enhancements in the thermoelectric power of alloys of lead[40] and aluminum[41].

This Experiment

In this experiment the difference in thermoelectric emf between a well-annealed rolled foil and a well-annealed wire was measured as a function of temperature from 4.2 ^{o}K to 333 ^{o}K, and the difference in thermoelectric power between the foil and the wire was determined.

The high temperature data is used to determine the values of U and V for each of the three noble metals. These values are then compared to those predicted by Robinson[9] in Chapter IV.

The low temperature data is explained by the effect of minute concentrations of un-oxydized iron. Analysis indicates that the thermoelectric size effect may provide a unique method of determining magnetic impurity concentrations of less than one part per million (ppm) in the noble metals.

Cold rolled foils were used to permit adequate annealing.

A detailed theoretical discussion of each effect is presented in Chapter II.

CHAPTER II

THEORY

High Temperature Thermoelectric Size Effect

At high temperatures the phonon-drag and second-order diffusion effects go to zero. This leaves the electronic thermoelectric power as the only remaining contribution to the absolute thermoelectric power.

We have seen that the electronic thermoelectric power of a pure metal is given by

$$S_e^o = \frac{\pi^2 k_B^2 T}{3e\epsilon_F} \{U+V\}_{\epsilon_F} \quad . \tag{15}$$

The parameters U and V were defined in Chapter I as

$$U = \frac{\partial \ell n \ell(\epsilon)}{\partial \ell n \epsilon} \quad \text{and} \quad V = \frac{\partial \ell n A(\epsilon)}{\partial \ell n \epsilon} \quad , \tag{16}$$

where ℓ is the mean free path, A the area of a constant energy surface, and ϵ the energy of the conduction electrons.

Huebener has shown[10] that U can be determined experimentally by measuring the influence of specimen size on the electronic thermoelectric power. The electrical resistivity, ρ, of thin wires and foils is larger than the resistivity, ρ_o, of the bulk material due to the scattering of electrons at the specimen surface.

Sondheimer[35] has calculated this increase in resistivity and found that for a cylindrical wire

$$\Delta\rho \equiv \rho - \rho_o = (\frac{3}{4\kappa})\rho_o \tag{17}$$

and for a foil

$$\Delta\rho \equiv \rho - \rho_o = (\frac{3}{8\kappa})\rho_o \ . \tag{18}$$

Here $\kappa = a/\ell$, where a is the diameter of the wire or the thickness of the foil. In Eqs. (17) and (18) it is assumed that $\kappa >> 1$ and that the electrons are scattered diffusely from the specimen surface. The electrical resistivity difference between a foil of thickness a_1 and a cylindrical wire of diameter a_2, caused by the electron scattering at the surface, is[10]

$$\Delta\rho \equiv \rho^{foil} - \rho^{wire} = \frac{3}{4}\,(\frac{1}{2a_1} - \frac{1}{a_2})\rho_o\ell \ . \tag{19}$$

Here ℓ is the average value over the Fermi surface of the electron mean-free path.

The change in the electronic thermoelectric power due to additional scattering events in the bulk material, which cause a resistivity increase $\Delta\rho$, is given by[42]

$$\Delta S_e \equiv S_e - S_e^o = \frac{S_e^o}{(\rho_o/\Delta\rho)+1}\left\{\frac{\partial \ell n \Delta\rho/\partial\varepsilon}{\partial \ell n \rho_o/\partial\varepsilon} - 1\right\}_{\varepsilon_F} \ . \tag{20}$$

Here S_e is the electronic thermoelectric power of the material, whose electrical resistivity is increased by $\Delta\rho$ due to the additional

electron scattering events. In the derivation of Eq. (20) the following assumptions are required:

(1) The additional scattering of electrons which causes the resistivity increase $\Delta\rho$, and all other electron scattering events in the crystal are independent of each other (Matthiessen's rule). i.e.

$$\rho = \rho_o + \Delta\rho \quad . \tag{21}$$

(2) The heat which is transported by the conduction electrons is independent of other heat transporting mechanisms (phonons).

(3) The electrical conductivity and the electronic component of the thermal conductivity are determined by the same relaxation time (Wiedemann-Franz Law).

The electronic thermoelectric power of a pure metal is given by[2]

$$S_e^o = \frac{\pi^2 k_B^2 T}{3e} \left\{\frac{\partial \ell n \rho_o}{\partial \varepsilon}\right\}_{\varepsilon_F} . \tag{22}$$

Inserting Eqs. (19) and (22) into Eq. (20), and with the relation $\Delta\rho << \rho_o$, we obtain for the difference between the electronic thermoelectric power of a foil of thickness a_1 and a wire of diameter a_2

$$\Delta S_e \equiv S_e^{foil} - S_e^{wire} = \left(\frac{1}{2a_1} - \frac{1}{a_2}\right) \frac{\pi^2 k_B^2 T}{4e\varepsilon_F} \left\{\frac{\partial \ell n \ell(\varepsilon)}{\partial \ell n \varepsilon}\right\}_{\varepsilon_F} . \tag{23}$$

As seen from Eq. (23) measurements of the size effect on the electronic component of the thermoelectric power yield information on the quantity U. Using Eq. (15) and a knowledge of S_e^o/T at high temperatures we can then get an estimate of the quantity V.

Low Temperature Thermoelectric Size Effect

Effect of Iron Impurities.

The presence of magnetic impurities, mainly iron, in the noble metals requires that a correction be made to the low temperature electronic thermoelectric power as suggested by Kondo.[33,43] It has the form of Eq. (11) which agrees with experimental data for dilute alloys of iron in the noble metals. Thus the intrinsic thermoelectric power of iron in the noble metals is given by

$$S_{Fe} = S_o \frac{T}{T+T_o} \quad , \tag{24}$$

where S_o and T_o are constants.

When more than one type of scattering is present, the resultant thermopower is the average of the intrinsic thermopowers of the components weighted according to the expression[44]

$$S = \frac{\sum_i \rho_i S_i}{\sum_i \rho_i} \tag{25}$$

ρ_i is the resistivity due to the ith component of the scattering present and S_i its thermoelectric power. In the derivation of Eq. (25) it is required that Matthiessen's rule and the Wiedemann-Franz Law are valid. In the present case let us consider the electronic thermoelectric power of the pure metal S_1, the electronic thermoelectric power due to surface scattering S_2, and the electronic thermoelectric power due to magnetic impurities S_3, and their respective resistivities.

$$S = \frac{\rho_1 S_1}{\rho} + \frac{\rho_2 S_2}{\rho} + \frac{\rho_3 S_3}{\rho} \quad , \tag{26}$$

where $\rho = \rho_1 + \rho_2 + \rho_3$. Defining

$$\rho_{SE} = \rho_1 + \rho_2 \tag{27}$$

we can rewrite Eq. (26) in the following form,

$$\begin{aligned} S &= \frac{\rho_1+\rho_2}{\rho} \left(\frac{\rho_1 S_1}{\rho_1+\rho_2} + \frac{\rho_2 S_2}{\rho_1+\rho_2}\right) + \rho_3 S_3 \\ &= \frac{\rho_{SE}}{\rho} S_{SE} + \frac{\rho_3 S_3}{\rho} \quad , \end{aligned} \tag{28}$$

where we have defined

$$S_{SE} = \frac{\rho_1 S_1}{\rho_1+\rho_2} + \frac{\rho_2 S_2}{\rho_1+\rho_2} \quad . \tag{29}$$

S_{SE} is the size-effect electronic thermoelectric power you would measure in a foil or wire separately.

The difference in the electronic component of the thermoelectric power between a foil and a wire can now be calculated.

$$\Delta S \equiv S^f - S^w \tag{30}$$

$$\begin{aligned} &= \frac{\rho^f_{SE}}{\rho^f} S^f_{SE} - \frac{\rho^w_{SE}}{\rho^w} S^w_{SE} + \frac{\rho^f_3}{\rho^f} S^f_3 - \frac{\rho^w_3}{\rho^w} S^w_3 \\ &= (S^f_{SE} - S^w_{SE}) + \frac{\rho^f_3}{\rho^f} (S^f_3 - S^f_{SE}) - \frac{\rho^w_3}{\rho^w} (S^w_3 - S^w_{SE}) \\ &= \Delta S_{SE} + \frac{\rho^f_3}{\rho^f} (S^f_3 - S^f_{SE}) - \frac{\rho^w_3}{\rho^w} (S^w_3 - S^w_{SE}) \end{aligned} \tag{31}$$

ΔS_{SE} is the size effect electronic thermoelectric power one would measure if no other scattering events were present. The resistivity, ρ_3, and electronic thermoelectric power, S_3, due to magnetic impurities are a property of the impurity and not of the sample configuration. Thus, $S_3^w = S_3^f = S_3$ and $\rho_3^w = \rho_3^f = \rho_3$. Equation (31) then becomes,

$$\Delta S = \Delta S_{SE} + \rho_3 \left[\frac{(S_3 - S_{SE}^f)}{\rho^f} - \frac{(S_3 - S_{SE}^w)}{\rho^w}\right] . \qquad (32)$$

We take the form of S_3 from Eq. (24) and experimentally we know that $S_o \simeq 14\ \mu V/^oK$[43]. Thus,

$$S_3 = S_o \frac{T}{T+T_o} \simeq 14\ \mu V/^oK \frac{T}{T+T_o} .$$

We also know that

$$\frac{S_{SE}^f}{T} \simeq \frac{S_{SE}^w}{T} \simeq \frac{S_e^o}{T} \simeq 0.007\ \mu V/^oK^2\ (10).$$

We therefore can neglect S_{SE}^f and S_{SE}^w in Eq. (32). Thus,

$$\Delta S = \Delta S_{SE} + \rho_3 S_3 \left(\frac{1}{\rho^f} - \frac{1}{\rho^w}\right) . \qquad (33)$$

An estimate (see below) of ΔS_{SE} at low temperatures yielded a value of the order of $0.01\ \mu V/^oK$. It will be ignored for the simplicity of the following calculation. Thus,

$$\Delta S = \rho_3 S_3 \left(\frac{1}{\rho^f} - \frac{1}{\rho^w}\right)$$

$$= \rho_3 S_o \frac{T}{T+T_o} \left(\frac{1}{\rho^f} - \frac{1}{\rho^w}\right) . \qquad (34)$$

This form will be used to analyze the observed results in the low temperature region.

We note at this point that the relevant theory for the analysis of all the experimental data has been developed. For clarity the reader may want to turn to Chapter III. The remaining parts of Chapter II discuss other current theories of thermoelectric power which were considered to explain the low temperature data. These theories gives contributions that are definitely secondary to the contribution of magnetic impurities.

Change in the Phonon-Drag Thermoelectric Power.

The phonon-drag thermoelectric power of a pure metal, S_o^g, can be expressed as a superposition of contributions from each phonon present in the metal and can be written as[45,46]

$$S_g^o = \sum_j \int s_g(\bar{q},j) d^3q \quad . \tag{35}$$

Here j is the polarization and $\bar{q}$ the wave vector of the phonon. The quantity $s_g(\bar{q},j)$ is the phonon-drag thermoelectric power associated with the phonons $\bar{q},j$. The change of the phonon-drag thermoelectric power due to the phonon scattering at the crystal surface is given by Huebener[42] as

$$\Delta S_g^{SE} = S_g - S_g^o = - \sum_j \int \frac{s_g(\bar{q},j)}{[\lambda_B/\lambda_o(\bar{q},j)]+1} d^3q \quad . \tag{36}$$

Here λ_B is the phonon mean free path for boundary scattering and $\lambda_o(\bar{q},j)$ is the phonon mean free path in the bulk material. In the

derivation of Eq. (36) the following assumptions are required:

1. The phonon scattering at the surface and all other phonon scattering events are independent (Matthiessen's rule).

2. The heat which is transported by the phonons is independent of the heat transported by electrons.

The boundary scattering of phonons is analogous to the boundary scattering of electrons. Therefore, the results of Sondhiemer[35] for electrons can be used directly to describe the boundary scattering of phonons. We find that the phonon mean free path for the boundary scattering in a foil of thickness a is

$$\lambda_B^{foil} = \frac{8a}{3} , \tag{37}$$

and the phonon mean free path for the cylindrical wire of diameter a is,

$$\lambda_B^{wire} = \frac{4a}{3} . \tag{38}$$

In Eqs. (37) and (38) it is assumed that $\lambda_B >> \lambda_o$ and that the phonons are scattered diffusely at the specimen surface.

Equations (37) and (38) show us that λ_B is independent of the wave vector and the polarization of a phonon, but the bulk mean free path, λ_o, is a function of $\bar{q}$ and j. In a rigorous treatment, ΔS_g^{SE} must be represented by an integral over $\bar{q}$ and a sum over j, as seen in Eq. (36). The calculation of ΔS_g^{SE} may be simplified by dropping the differentiation between phonons with different polarizations and by replacing the sum over j by the factor 3. In the integration over all phonons the phonon frequency spectrum may be cut

off at the Debye frequency. Further, dispersion may be neglected.

The analysis of ΔS_g^{SE} along the lines given above is desirable, but rather difficult. This is due to the uncertainties in determining the function $s_g(\bar{q})$. On the other hand, the bulk phonon mean free path, λ_o, may not depend very strongly on the wave vector.[47] Therefore, Huebener[18] has simplified the treatment even further by the substitution of an average phonon frequency around which the phonon distribution is concentrated at any given temperature for the phonon frequency spectrum. Thus, Eq. (22) is

$$\Delta S_g^{SE} = - \frac{S_o^g}{(\lambda_B/\lambda_o)+1} \quad . \tag{39}$$

Using Eq. (39) in combination with Eqs. (37) and (38) the difference between the phonon-drag thermoelectric power of a foil of thickness a_1 and a cylindrical wire of diameter a_2 is found to be

$$\Delta S_g^{SE} \equiv S_g^{foil} - S_g^{wire} = - S_g^o \left[\frac{1}{(8a_1/3\lambda_o)+1} - \frac{1}{(4a_2/3\lambda_o)+1}\right]. \tag{40}$$

With the relation $\lambda_B >> \lambda_o$, which was assumed in the derivation of Eqs. (37) and (38), we obtain

$$- \frac{\Delta S_g^{SE}}{S_g^o} = \frac{3}{4} \left(\frac{1}{2a_1} - \frac{1}{a_2}\right)\lambda_o \quad . \tag{41}$$

As is seen, measurements of the size effect on the phonon-drag thermoelectric power yield information on the mean free path, λ_o, of the dominant phonon mode in the bulk material.

At temperatures above the phonon-drag peak λ_o is mainly limited by phonon-phonon umklapp processes. If phonon-phonon umklapp processes are the main source of the lattice thermal resistance, λ_o has the form[47]

$$\lambda_o = Ae^{T^*/T} \tag{42}$$

below the Debye temperature. Here T* is about half the Debye temperature and A is a constant. Equation (41) is then given by

$$-\frac{\Delta S_g^{SE}}{S_g^o} = \frac{3}{4}\left(\frac{1}{2a_1} - \frac{1}{a_2}\right)Ae^{T^*/T} \quad . \tag{43}$$

Equation (43) should be valid between the temperature of the phonon-drag peak and the Debye temperature.

Using T* as half the Debye temperature and taking $A = 1.1 \times 10^{-5}$ mm from the work of Huebener on platinum, we have estimated that in the noble metals $|\Delta S_g^{SE}| \simeq 0.01$ $\mu V/^oK$ and can be neglected as an explanation of the 0.3 $\mu V/^oK$ peak seen in this experiment at low temperatures.

We saw from Eqs. (12) and (13) that the phonon-drag thermoelectric power should be reduced in absolute magnitude by the addition of new scattering events for phonons. Recent experiments[48-50] have shown that the magnitude of S_g can increase and even, in some cases, change its sign due to the admixture of impurities. An explanation of these anomoulous results in terms of the anisotropy of the electron scattering has been suggested.[36,49]

Bailyn[51] has considered the phonon-drag thermoelectric power for the highly anisotropic Fermi surface, as in most metals, in detail. He assumed a relaxation time that was not a constant, but rather a function of position on the Fermi surface. He showed that, after dividing the Fermi surface into different regions j, the total phonon drag thermoelectric power can be written in the form

$$S_g = \sum_j \left(\frac{\sigma_j}{\sigma}\right) S_{gj} \quad . \tag{44}$$

Here, σ_j and S_{gj} are the electrical conductivity and phonon-drag thermoelectric power of region j respectively. Equation (44) is particularly useful if the Fermi surface can be divided such that σ_j is approximately constant for each region. The contributions S_{gj} from the different parts of the Fermi surface can differ strongly in both magnitude and sign. In a sufficiently pure metal the factor σ_j/σ is determined by the electron-phonon interaction. However, in a dilute alloy, at low temperatures, the factor σ_j/σ can be given by the electron-impurity interaction. If the electron scattering for the two scattering mechanisms varies differently over the Fermi surface, the factors σ_j/σ in the pure metal can be quite different from those in a dilute alloy. Thus, the low temperature phonon-drag thermoelectric power can depend very sensitively on the electron scattering mechanism. A detailed discussions of these effects in the noble metals has been given by Dugdale and Bailyn[36]. They distinguish three regions which are the main contributors to the phonon-drag thermoelectric power at low temperatures. These are:

(1) the convex belly regions, (2) the concave belly regions, and (3) the neck regions. It is often assumed that apart from the necks, the Fermi surfaces of the noble metals are nearly spherical. There are, however, substantial concave regions which are particularily conspicuous in Cu and Au.

The sum of the phonon-drag thermoelectric power over the regions j can be expressed as three terms corresponding to the convex belly (cv), concave belly (cc), and neck (n) regions. Thus,

$$S_g = \frac{\sigma_{cv}}{\sigma} S_{g,cv} + \frac{\sigma_{cc}}{\sigma} S_{g,cc} + \frac{\sigma_n}{\sigma} S_{g,n} \quad . \tag{45}$$

They found that the electron-phonon interaction affects the S_{gj} and the electron-impurity interaction affects the σ_j/σ. This means that the S_{gj} depend upon the properties of the host material and that the σ_j/σ reflect the effect of adding impurities. Following the analysis of Dugdale and Bailyn it is seen that $S_{g,n}$ is entirely dominant in the case of Ag, $S_{g,cc}$ is slightly larger in Au, and $S_{g,n}$ and $S_{g,cc}$ contribute to S_g in Cu.

Dugdale and Bailyn have examined the effects of alloying with various types of impurities on the σ_j/σ and the resulting S_g.

While their approach does not yield a quantitative result it has been used as a possible explanation of the anomalous results observed in the phonon-drag thermoelectric power in metals. It is not believed, however, that the results are applicable to the size effect on the phonon-drag thermoelectric power of the noble metals. Since it was found that the main contribution to S_g is different in

each of the noble metals it would seem that the size effect on the phonon-drag thermoelectric power would differ in each of the noble metals. This, however, has not been the case in the present investigation.

Change in the Electronic Thermoelectric Power.

In 1970 Nielson and Taylor[38,39] extended the theory of the electronic thermoelectric power in both pure metals and dilute alloys. Their results allow an interpretation of low temperature thermoelectric measurements that relies less on the phenomenom of phonon-drag than has previously been the case.

From Eq. (2) we have that the electronic thermoelectric power of a metal is given by

$$S_e^o = \frac{\pi^2 k_B^2 T}{3e} \left\{\frac{\partial \ell n \sigma(\varepsilon)}{\partial \varepsilon}\right\}_{\varepsilon_F} . \tag{46}$$

It is often convenient to express Eq. (46) in terms of a dimensionless thermopower parameter ξ, given by

$$\xi = \left\{\frac{\partial \ell n \sigma(\varepsilon)}{\partial \ell n \varepsilon}\right\}_{\varepsilon_F} . \tag{47}$$

Then,

$$S_e^o = S^o \xi, \qquad S^o = \frac{\pi^2 k_B^2 T}{3e\varepsilon_F} . \tag{48}$$

We can write the conductivity as in Eq. (3)

$$\sigma(\varepsilon) \alpha v^2(\varepsilon) \tau(\varepsilon) N(\varepsilon) . \tag{49}$$

In a system of free electrons, both $v(\varepsilon)$ and $N(\varepsilon)$ are proportional to $\varepsilon^{\frac{1}{2}}$. Thus, we have

$$\xi = \frac{3}{2} - \left\{\frac{\partial \ell n(1/\tau)}{\partial \ell n \varepsilon}\right\}_{\varepsilon_F} . \qquad (50)$$

Nielson and Taylor found that second order corrections to the T-matrix for electron scattering involving intermediate virtual phonon states result in strongly energy dependent corrections to τ, and thus greatly influence the thermoelectric power. What results are contributions to the electronic thermoelectric power of the same order of magnitude and position which have previously been ascribed to phonon-drag.

The central variable in this theory is psuedopotential difference between the host and the impurity, P. We tried to adapt this theory to surface scattering by fitting the thermoelectric data by varying P. This led to an anomalously high value for P of about 1.8 rydbergs. This is too large to be explained by surface scattering, but indicates the presence of an abnormally effective scattering center, namely a magnetic impurity.

CHAPTER III

THE EXPERIMENT

Sample Preparation

The samples were prepared from 99.999% pure wire. Gold wire was obtained from Sigmund Cohn Corporation[1], copper wire from A. D. Mackay, Inc.[2], and silver wire from Ventron Alfa Products[3]. Foils with a thickness of 2.54×10^{-2} to 1.524×10^{-3} mm were manufactured from this wire by cold rolling. This was done by Microfoils[4]. The samples consisted of a thermocouple made from a foil and two 2.54×10^{-2} mm diameter wires. Before assembling, the components were acid etched, rinsed in distilled water, acetone, and finally methanol. Gold was etched in nitric acid, copper in a 25% nitric acid solution, and silver in hydrochloric acid. The sample and sample holder are illustrated in Fig. 1. The wires were bent and the sample spot welded together. The length of the foil between the hot and the cold junctions was about 9 cm. The foils were from 2 to 8 mm wide.

---

[1]Sigmund Cohn Corporation, Mount Vernon, New York.

[2]A. D. Mackay, Inc., New York, N. Y.

[3]Ventron Alfa Products, Beverly, Massachusetts

[4]Microfoils, Argonne, Illinois.

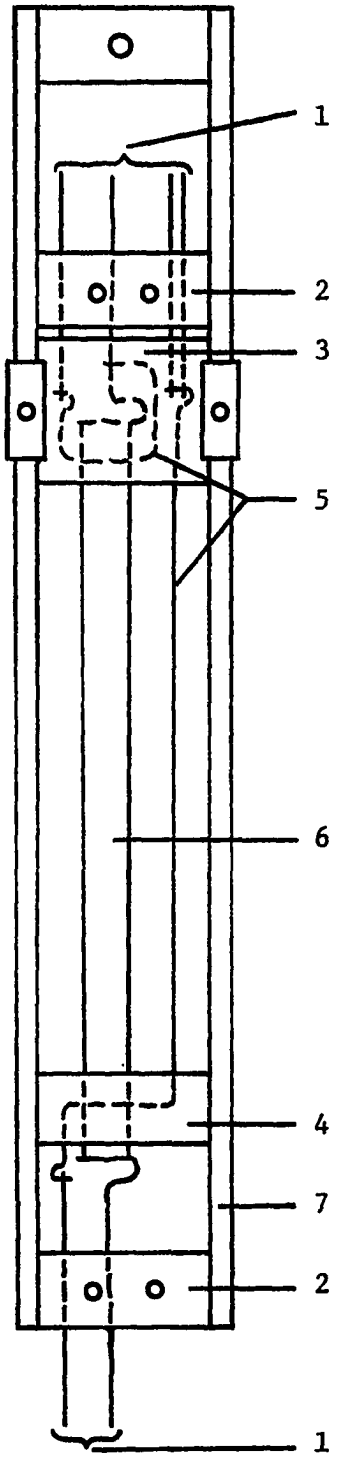

1. 0.0015" Support Leads
2. Phenolic Sample Clamps
3. Copper Heat Sink
4. Copper Heater Block
5. 0.0010" Sample Wires
6. Foil Sample
7. Stainless Steel Sample Frame

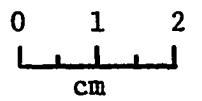

Figure 1. Sample holder and sample.

Annealing Techniques

The sample was placed on a high density alumina block for annealing. The alumina annealing block was used because it was found that it introduced the least contamination of several attempted alternatives. Measurement of the thermoelectric size effect requires a well-annealed specimen of high purity in order to detect the influence of the specimen surface only.

As mentioned before, all of the noble metals have a small percentage of iron present in commercially available wire. The most comprehensive work investigating the annealing procedures designed to remove the effect of iron is that of Fickett[52] on copper, and Ehrlich[53] on silver. The procedure is to anneal the sample in an oxidyzing atmosphere and measure the increase in the resistance ratio (RR), defined as the ratio of the resistance at room temperature to the resistance at 4.2 ^{o}K. It is thought[52] that the oxygen diffuses into the metal and combines with the iron to give iron oxide. This presents a less energy dependent scattering center than the iron. The problem is to find that combination of temperature, time, and pressure which will yield the largest value of the resistance ratio. A temperature of 800 ^{o}C was used because higher temperatures deformed the foils to a point where they could not be used. The largest resistance ratio was obtained in gold when samples were annealed for 30 hours at atmospheric pressure, and in copper when samples were annealed for 3 hours at a pressure of 1.5×10^{-4} torr. The 2.5×10^{-2} through 5.08×10^{-3} mm silver samples were annealed for 5 hours at a pressure of 1.5×10^{-4} torr. In thinner silver samples it was found

that this amount of annealing destroyed the foils. Thus, the 2.54×10^{-3} through 1.524×10^{-3} mm silver samples were annealed in a different manner. The wire portion of the sample was annealed at 800 °C for 5 hours at 1.5×10^{-4} torr. The foil portion of the sample was raised to 800 °C for a matter of minutes at a pressure of 1.5×10^{-4} torr. In each case the sample was cooled at a rate of less than 150 °C per hour. In the case of the thin silver samples this allowed the foil to be above 600 °C for about 2 hours.

The annealing was performed in a diffusion pump vacuum-tube furnace which was capable of an ultimate pressure of less than 1×10^{-6} torr. The temperature was contolled by a chromel-alumel thermocouple connected to a Leeds and Northrup Speedomax W controller recorder with Azar unit and Series 60 control. The pressure was read by a Phillips tube and controller. Air was introduced into the system, to obtain the desired pressure, by a small micrometer valve.

Sample Holder

The sample holder was patterned after that of Huebener[10]. It was constructed of thin-walled stainless steel tubing with brass end pieces. The heat sink, heater block, and specimen clamps are shown in Fig. 1. General Electric 7031 adhesive and insulating varnish was used as an electrical insulator on all metal parts.

Thermoelectric Emf Measurements

Thermoelectric emf measurements were carried out using a Guildline 9176-G nanovolt potentiometer in conjunction with a Guildline 9460-A photoelectric nanovolt amplifier and a Guildline 9461-A

galvonometer. Thermoelectric connections to the cryostat were made with Guildline type SCW low thermal wire, in order to minimize thermal emf's in the measuring circuit. The circuit is illustrated in Fig. 2.

Resistance Measurement

The standard four-probe technique was employed to make resistance measurements. Reversing the current leads and repeating the measurements eliminated the effects of thermal emf's. The current was measured across a Leed's and Northrup one-ohm standard resistor using a Leed's and Northrup K-4 potentiometer together with a Leed's and Northrup dc null-detector. The voltage was measured on the same instruments used for measuring thermoelectric emf's. This circuit is illustrated in Fig. 2.

Temperature Measurement

The temperature of the hot junction was measured by calibrated platinum and germanium resistors embedded in the heater block. The germanium resistor was used in the temperature range 4.2 ^{o}K to 100 ^{o}K, and the platinum resistor was used in the temperature range 77 ^{o}K to 333 ^{o}K. The resistors were symmetrically placed in the heater blocks and positioned within less than 1 mm of the hot junction. The heater consisted of two 125 ohm heaters of manganin wire wound concentrically around each heater block and resistor, and connected in series. The temperature was controlled and measured simultaneously by an A.C. resistance bridge and temperature controller.

In 1970 Ries and Moore[54] developed a solid state temperature control unit which is easily built, and has proven to be

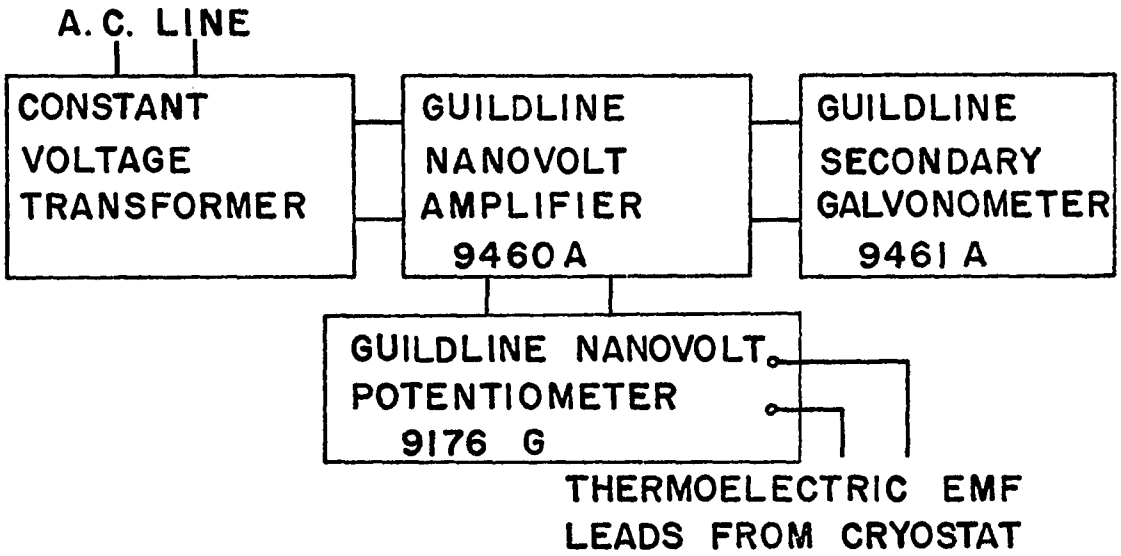

A. THERMOELECTRIC EMF MEASUREMENT

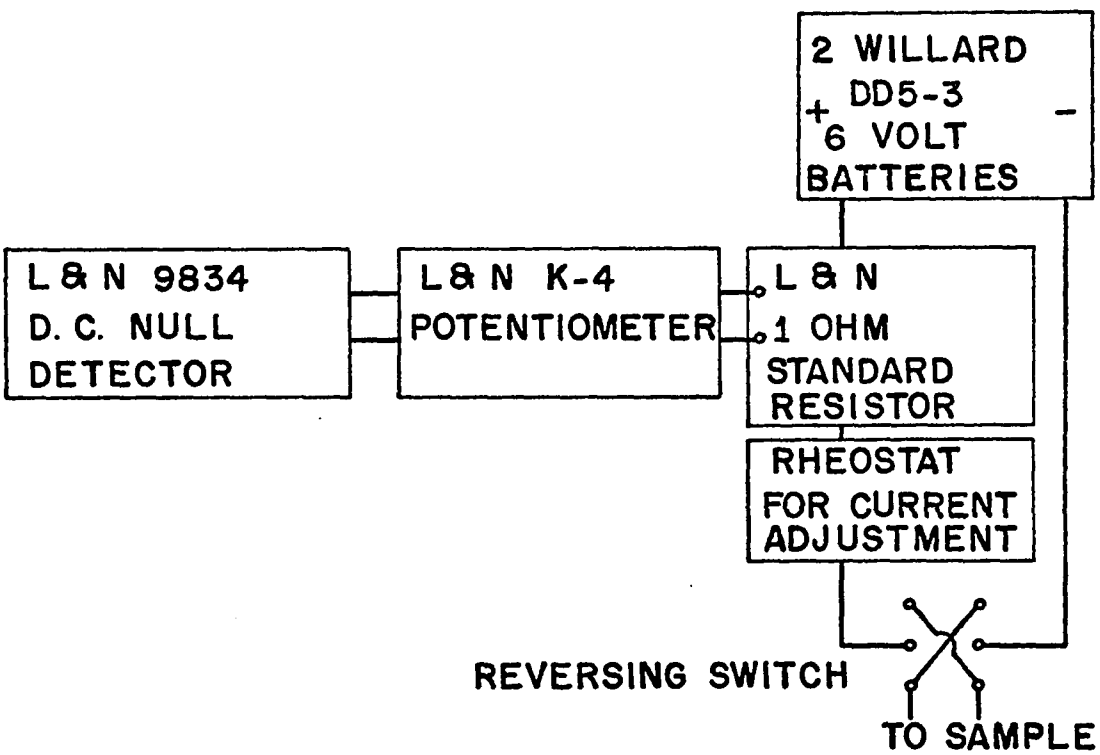

B. RESISTANCE MEASUREMENT

Figure 2.

dependable and accurate in its design range of 0.2 watts. In the present experiment it was found that much higher power levels were required. A modified version of the Ries and Moore controller was built which gives 2.5 watts to a 250 ohm heater and allows accurate control of the temperature in the range 0.03 ^{o}K to 300 ^{o}K. The controller is versatile, simple to operate, and very reliable. Under normal operating conditions it easily maintains constant temperature to within 1 part in 10^{4}.

The modifications required are in the controller section described by Ries and Moore. The increase in power was accomplished by the circuit in Fig. 3. The output from the phase sensitive detector, a PAR[1] Model 122 Lock-in Amplifier in conjunction with a PAR Model 112 X100 Preamplifier, is fed into the controller. R1 adjusts the amount of linear proportional feedback and R2 provides manual adjustment of the heater current. A1 sums the two signals and drives Q1 to furnish up to 100 ma to a 250 ohm heater. Diode D1 protects the output current meter against overload and S2 adjusts the sensitivity of the output current meter.

Two important points need to be made. First, the integrator used in the Ries and Moore controller was omitted. It can, however, be added at any time between points P1 and P2 if needed. Secondly, the variable 0-30 volt power supply allows one to preset the maximum current available to the heater. This flexibility has proven valuable in adapting the same controller to different cryogenic experiments.

---

[1]Princeton Applied Research Corp., Princeton, New Jersey.

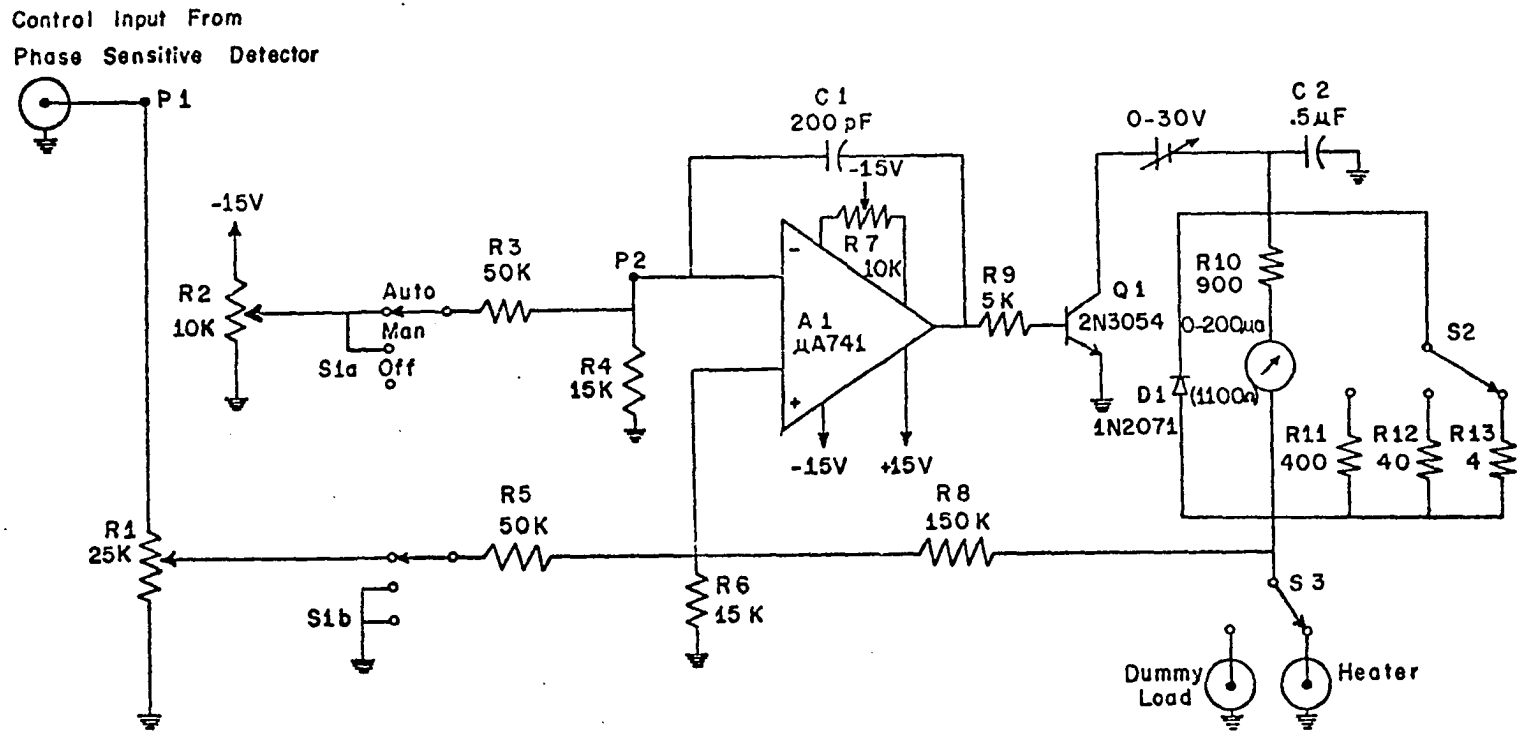

Figure 3. Schematic diagram of controller with modifications.

Experimental Procedure

After a sample was annealed for the proper length of time it was then cooled. The sample was transferred to the sample holder. It was necessary to do this in such a way as to introduce as little cold working as possible. To accomplish this the phenolic sample clamps were slipped under the sample into the grooves A and B in the alumina block, see Fig. 4. The sample holder was placed on top of the sample, the sample clamps screwed to the sample holder, the retaining wires cut, and the sample lifted off the annealing block. The other half of the heater block was attached and the sample holder was then mounted on the cryostat and the heat sink clamped into place. Silicon vacuum grease was used on the heater and heat sink clamping surfaces to the thermal contact. All of the leads were connected and the vacuum can bolted into place. The vacuum seal was made using an indium O-ring seal. At this point the cryostat was placed inside the dewars and a mechanical vacuum pump was used to evacuate the vacuum can. After thermal and pressure equilibrium were established, the room temperature resistance of the foil and the wire were measured. The cryostat was then cooled to 77.3 ^{o}K by adding a small amount of nitrogen gas to the inner dewar jacket to improve the heat transfer, evacuating the inner dewar and then back filling with helium gas, and introducing liquid nitrogen into the outer dewar. As a rule it took about eight hours for the temperature to come to equilibrium. With the cryostat at 77.3 ^{o}K the nitrogen temperature resistance of the foil and the wire was measured, after which the inner jacket was evacuated. Liquid helium was then transferred into

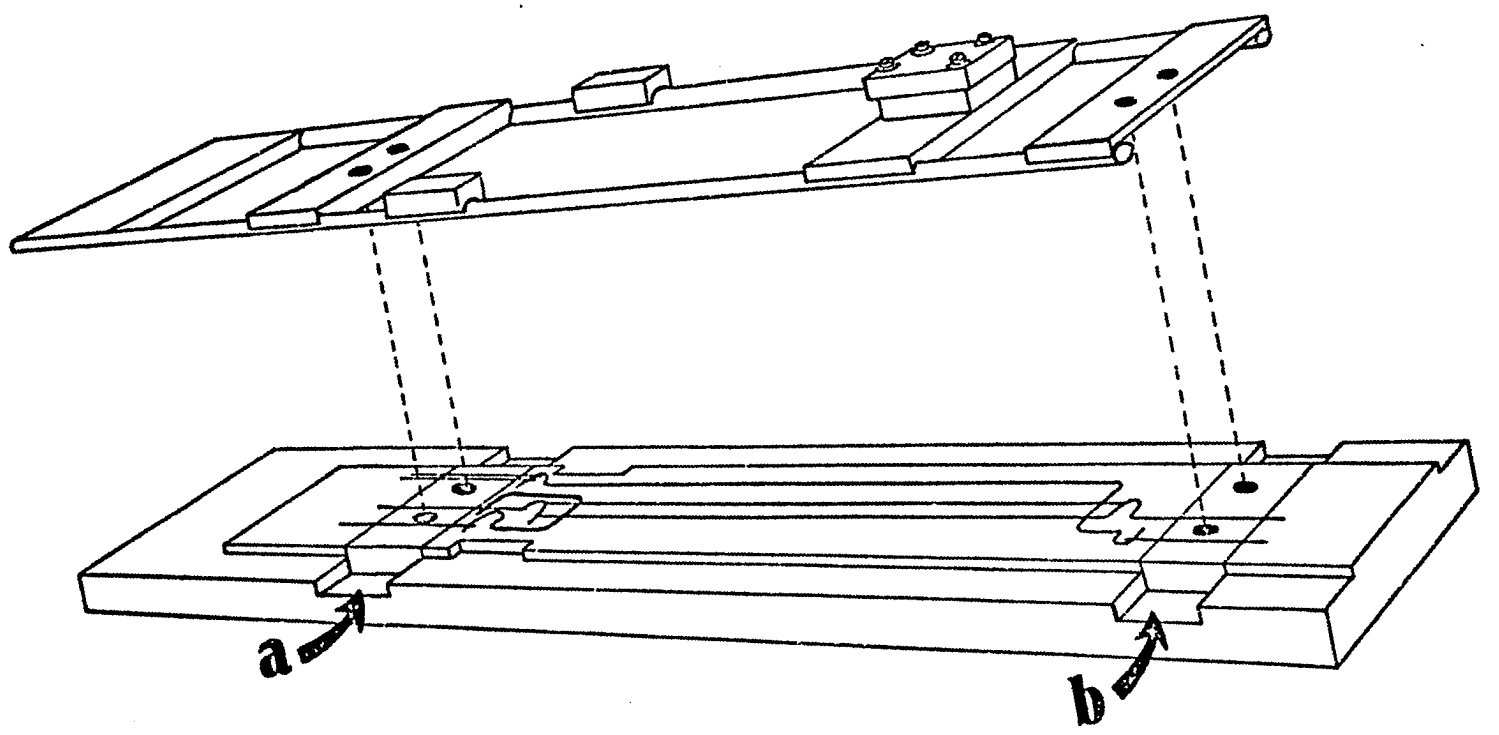

Figure 4. Perspective view indicating method of sample transfer from annealing block to sample holder.

the inner dewar to a height of ten inches above the top of the vacuum can. This provided helium for six to eight hours of measurements. It took from one to two hours for the temperature of the cryostat to again reach equilibrium. The helium temperature resistance of the foil and the wire was then measured.

The resistance ratio (RR) was computed for the sample and if it fell in a range predetermined by the previously mentioned annealing experiments, then the thermoelectric measurements proceeded. The thermoelectric emf measurements were made using the integral technique. One junction was maintained at 4.3 ^{o}K and the other raised in temperature. At each temperature the thermoelectric emf was measured. This was done over the range 4.2 ^{o}K to 100 ^{o}K with liquid helium in the inner dewar, and over the range 77.3 ^{o}K to 333 ^{o}K with liquid nitrogen in the inner dewar.

The temperature drift of the heat sink was checked with both liquid helium and liquid nitrogen in the inner dewar. The change in the temperature of the heat sink, with a maximum temperature gradient across the sample, was found to be less than 1 ^{o}K in each case.

The thermoelectric emf's were then differentiated yielding a point by point slope which is the change in the thermoelectric power between the foil and the wire as a function of temperature.

After completion of each experiment, the foil was cut off, and the length and width of the foil were measured with a micrometer microscope. The average thickness of the foil was then determined from its weight using the density of the particular material.

CHAPTER IV

RESULTS AND ANALYSIS

Thermoelectric Power Curves for Gold, Copper, and Silver

The difference in the thermoelectric power between a well-annealed foil and a well-annealed wire was found by differentiating the thermoelectric emf with respect to temperature. These results are given by the solid line curves in Figs. 5-10 for gold, Figs. 11-16 for copper, and Figs. 17-22 for silver. The important features of these results are the peak at about 14 ^{o}K, the rapid decrease in ΔS with increasing temperature after the peak, and the nearly constant negative value at temperatures in excess of 100 ^{o}K for gold. For copper the important features are the peak at 26-30 ^{o}K, the slow decrease in ΔS with increasing temperature after the peak, and the fact that at high temperatures a constant value is not reached as in the case of gold. For silver the important features are the peak at about 20 ^{o}K, the rapid decrease in ΔS with increasing temperature after the peak, and the nearly constant positive value at temperatures in excess of 100 ^{o}K.

The dashed curves represent calculated values of ΔS based on the assumption of magnetic impurity scattering. These will be discussed in more detail below.

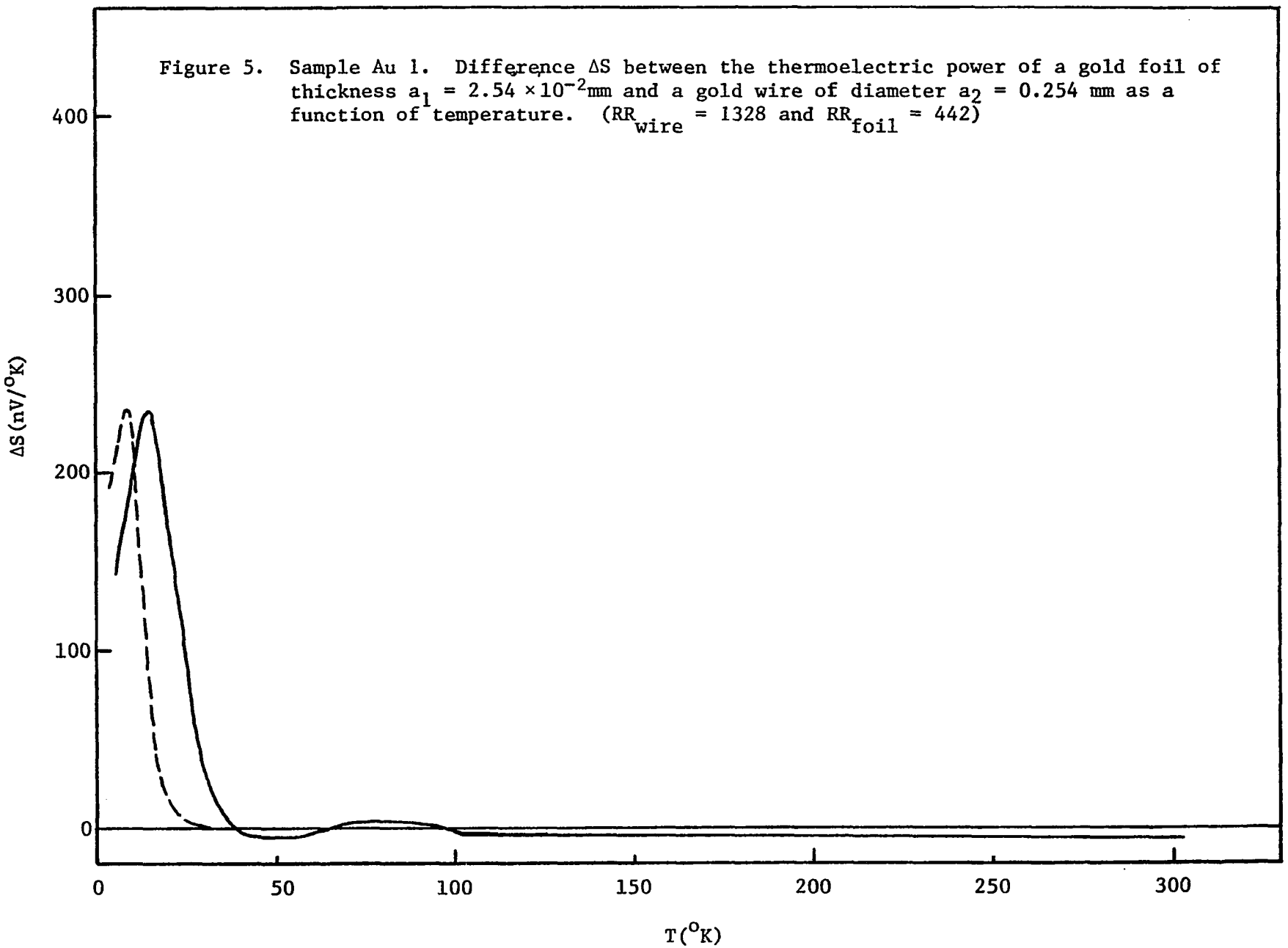

Figure 5. Sample Au 1. Difference ΔS between the thermoelectric power of a gold foil of thickness $a_1 = 2.54 \times 10^{-2}$mm and a gold wire of diameter $a_2 = 0.254$ mm as a function of temperature. ($RR_{wire} = 1328$ and $RR_{foil} = 442$)

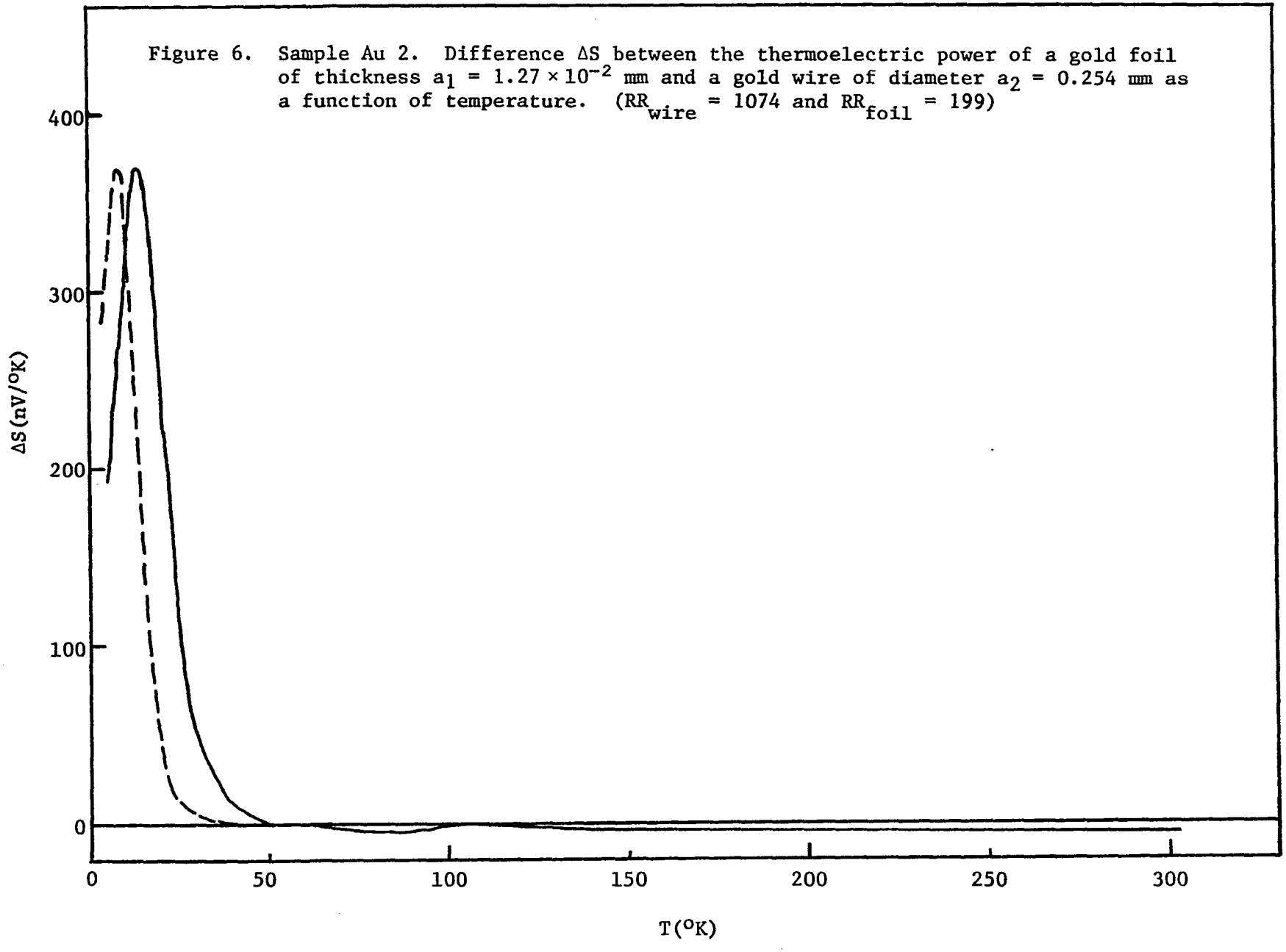

Figure 6. Sample Au 2. Difference ΔS between the thermoelectric power of a gold foil of thickness $a_1 = 1.27 \times 10^{-2}$ mm and a gold wire of diameter $a_2 = 0.254$ mm as a function of temperature. ($RR_{wire} = 1074$ and $RR_{foil} = 199$)

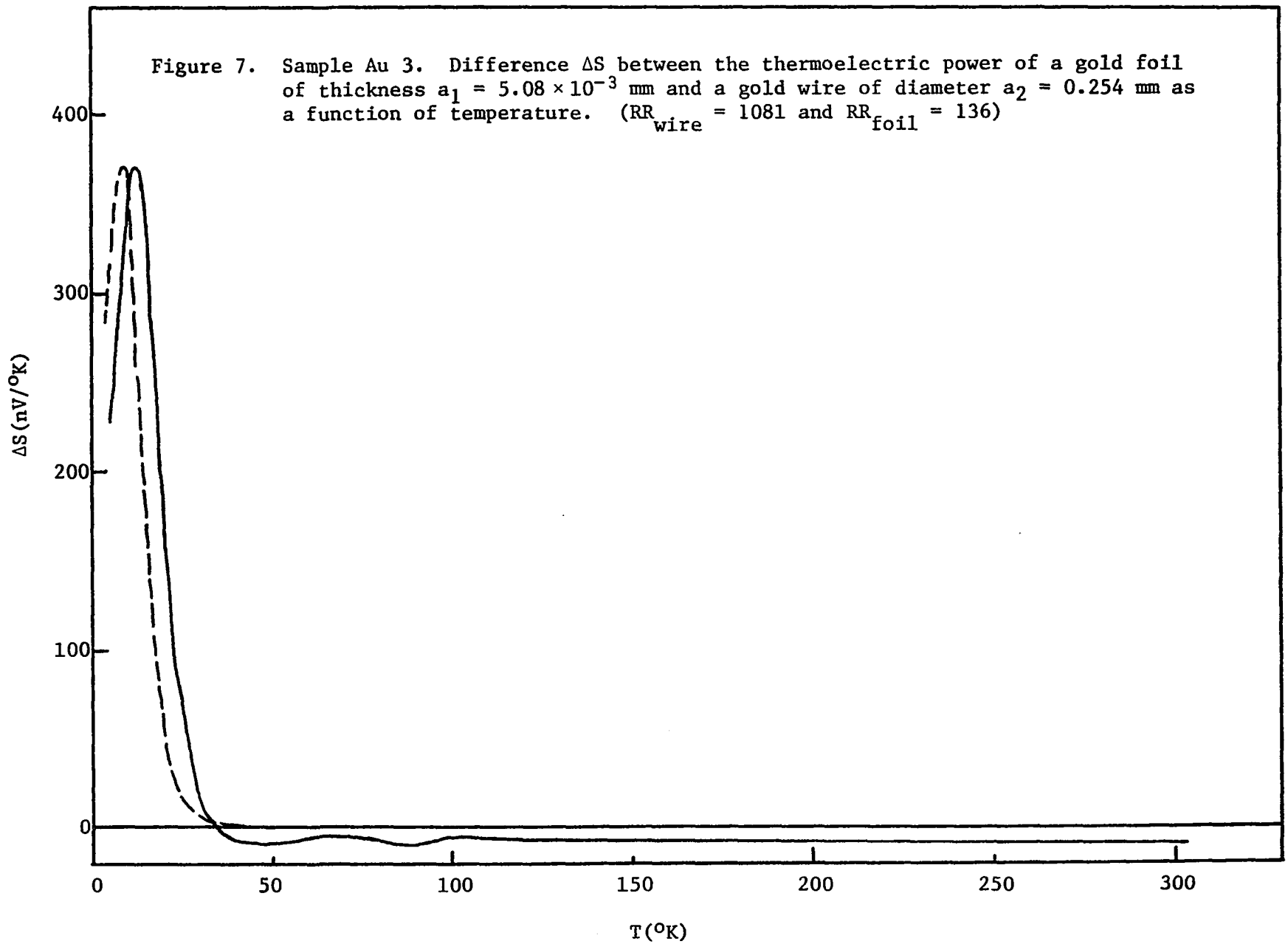

Figure 7. Sample Au 3. Difference ΔS between the thermoelectric power of a gold foil of thickness $a_1 = 5.08 \times 10^{-3}$ mm and a gold wire of diameter $a_2 = 0.254$ mm as a function of temperature. ($RR_{wire} = 1081$ and $RR_{foil} = 136$)

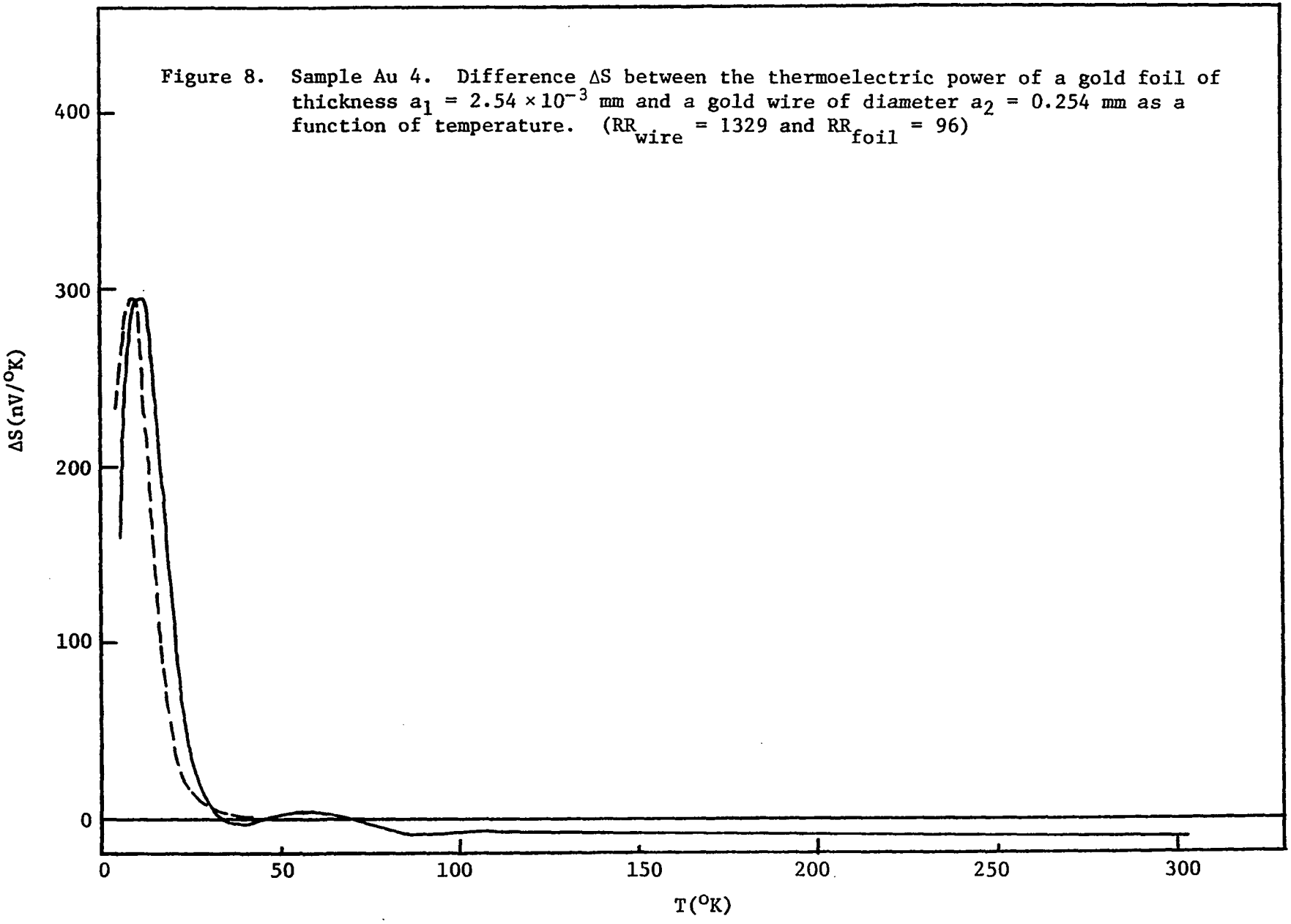

Figure 8. Sample Au 4. Difference ΔS between the thermoelectric power of a gold foil of thickness $a_1 = 2.54 \times 10^{-3}$ mm and a gold wire of diameter $a_2 = 0.254$ mm as a function of temperature. ($RR_{wire} = 1329$ and $RR_{foil} = 96$)

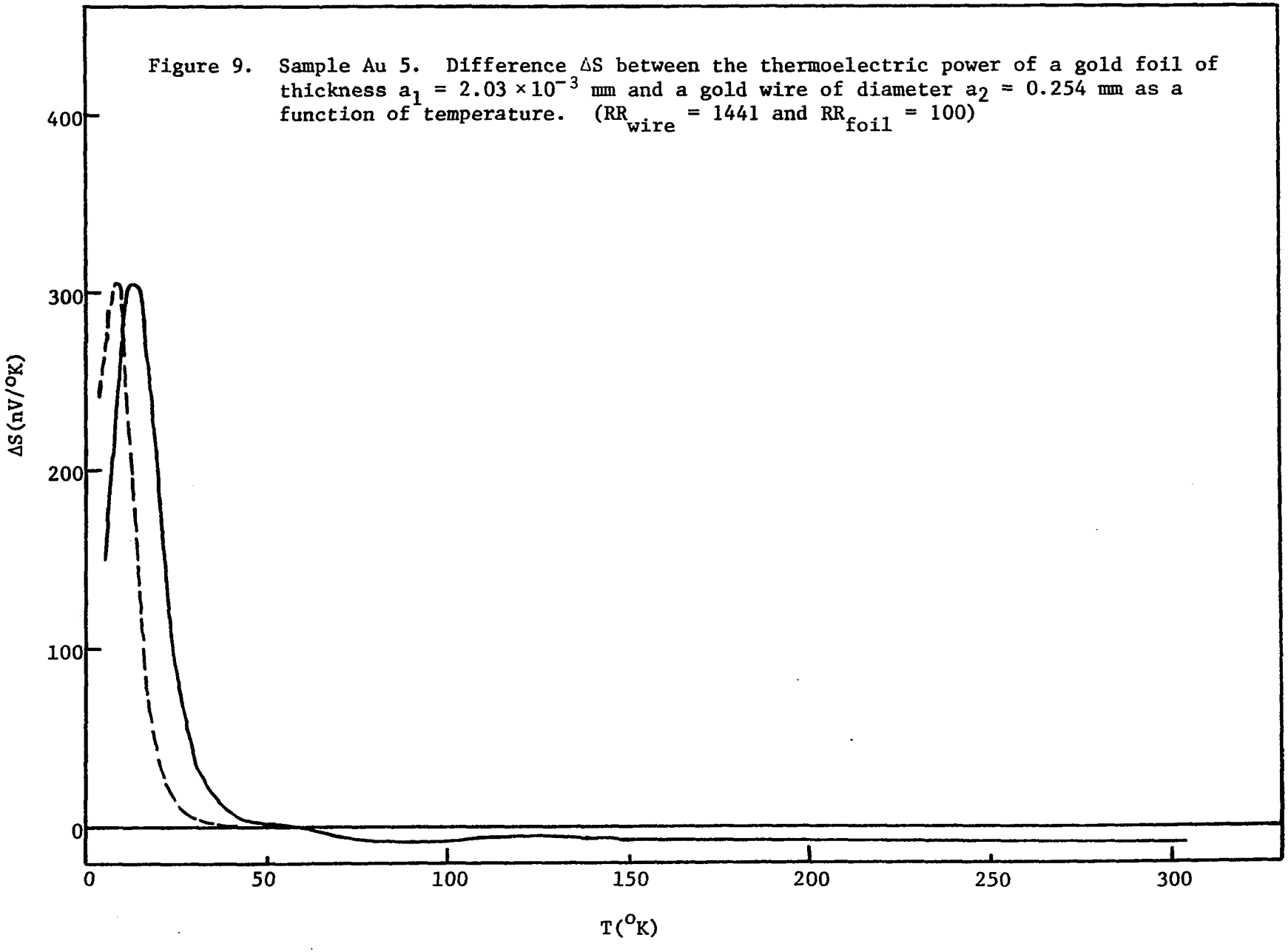

Figure 9. Sample Au 5. Difference ΔS between the thermoelectric power of a gold foil of thickness $a_1 = 2.03 \times 10^{-3}$ mm and a gold wire of diameter $a_2 = 0.254$ mm as a function of temperature. ($RR_{wire} = 1441$ and $RR_{foil} = 100$)

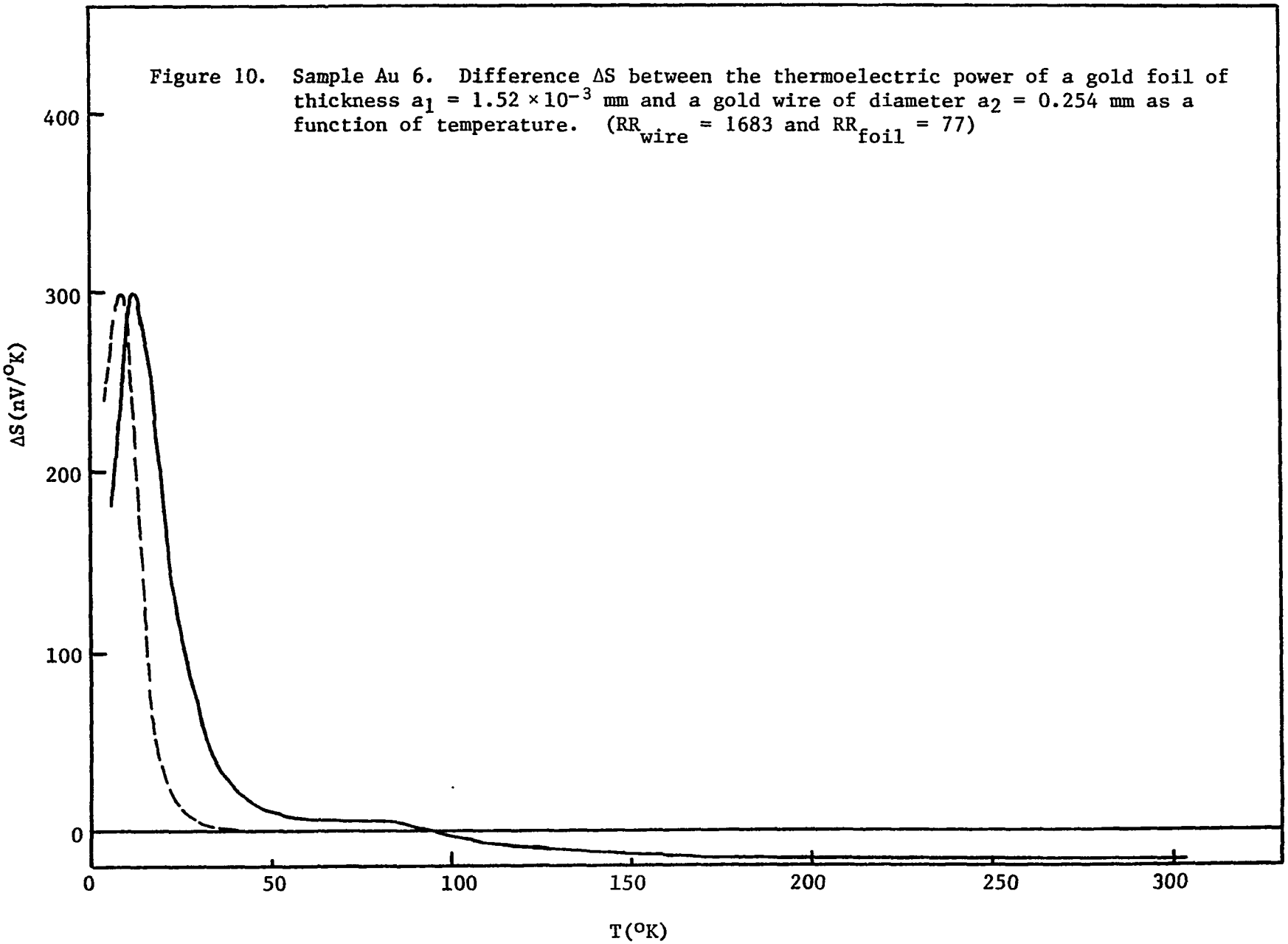

Figure 10. Sample Au 6. Difference ΔS between the thermoelectric power of a gold foil of thickness $a_1 = 1.52 \times 10^{-3}$ mm and a gold wire of diameter $a_2 = 0.254$ mm as a function of temperature. ($RR_{wire} = 1683$ and $RR_{foil} = 77$)

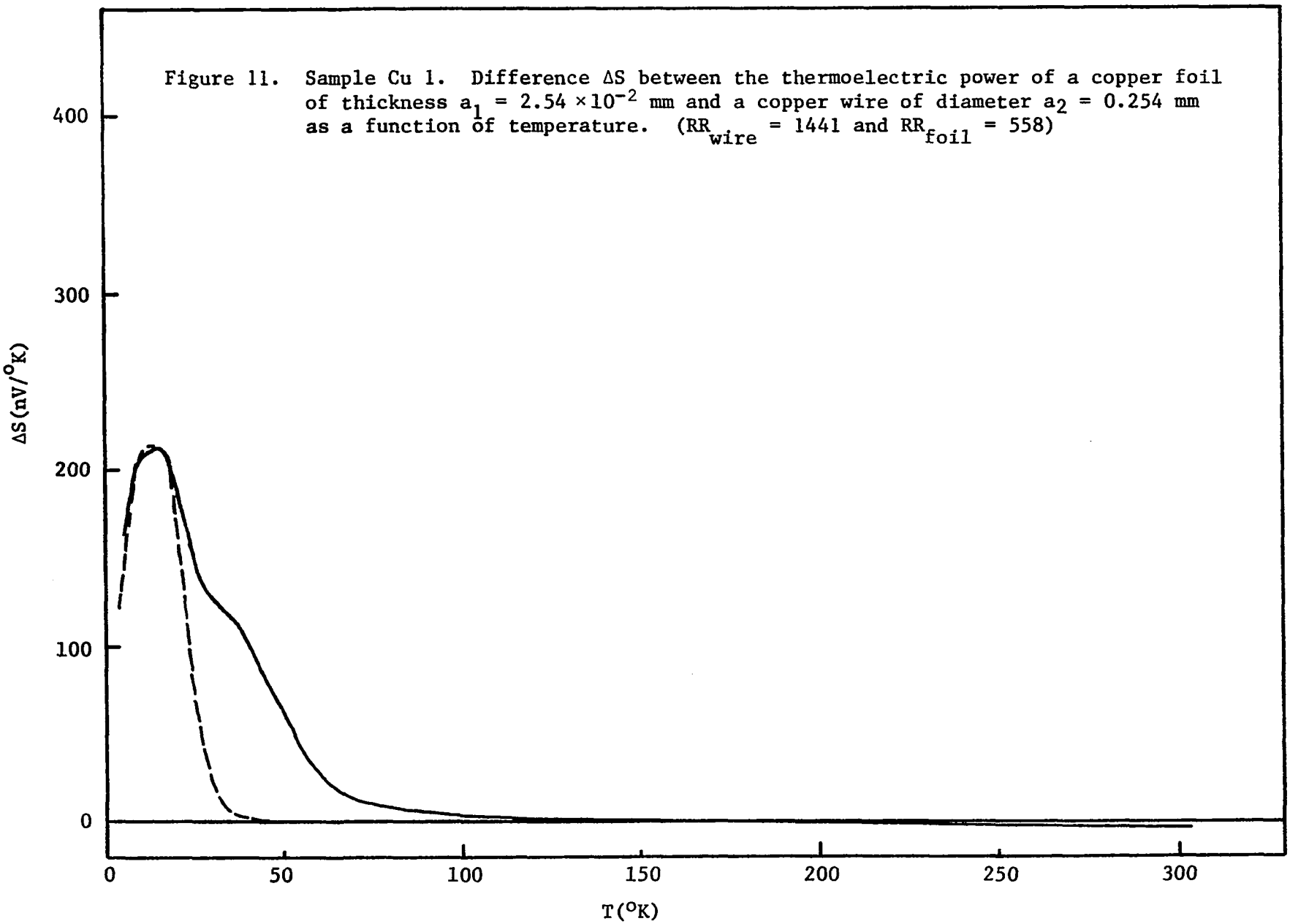

Figure 11. Sample Cu 1. Difference ΔS between the thermoelectric power of a copper foil of thickness $a_1 = 2.54 \times 10^{-2}$ mm and a copper wire of diameter $a_2 = 0.254$ mm as a function of temperature. ($RR_{wire} = 1441$ and $RR_{foil} = 558$)

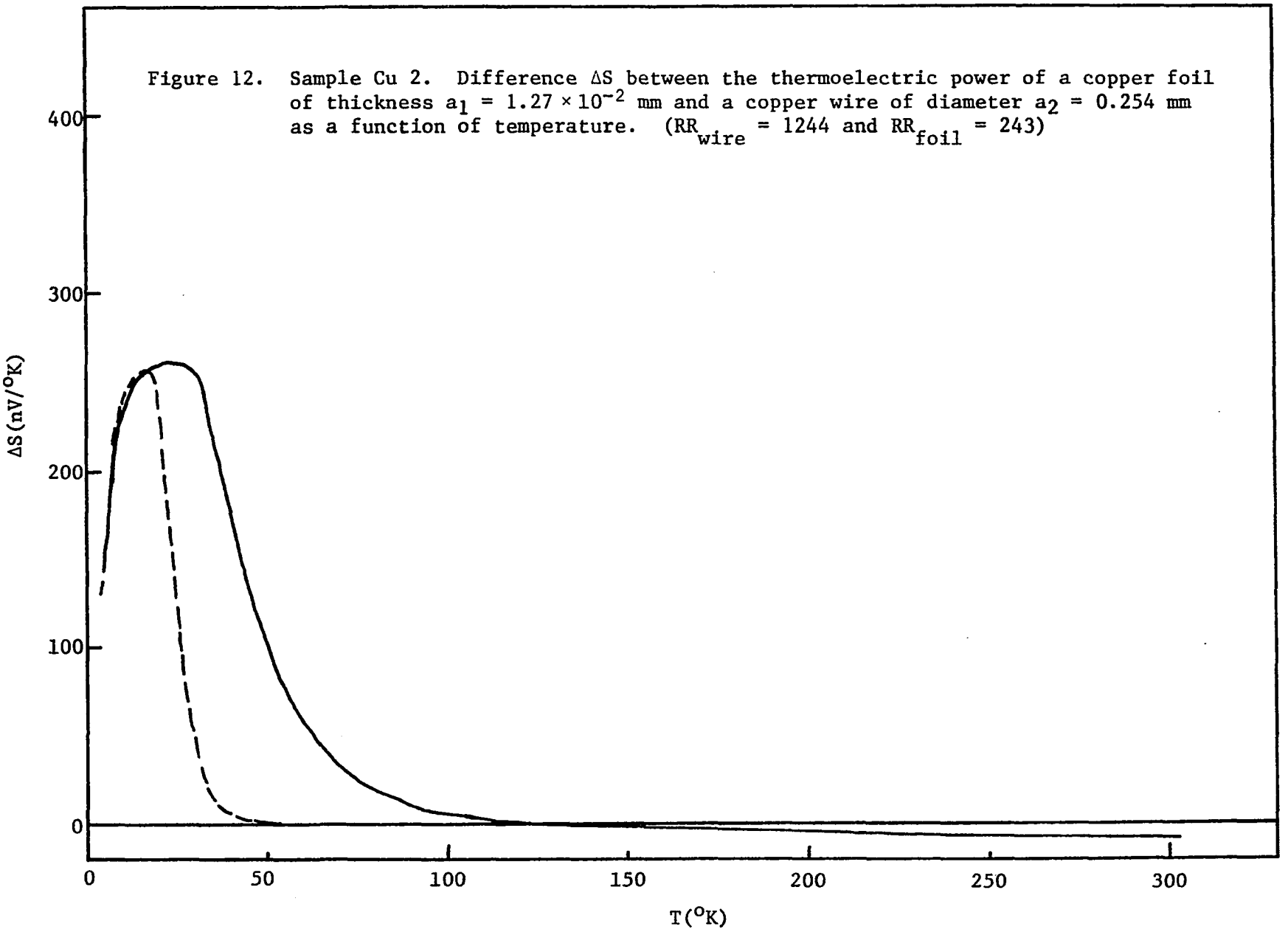

Figure 12. Sample Cu 2. Difference ΔS between the thermoelectric power of a copper foil of thickness $a_1 = 1.27 \times 10^{-2}$ mm and a copper wire of diameter $a_2 = 0.254$ mm as a function of temperature. ($RR_{wire} = 1244$ and $RR_{foil} = 243$)

Figure 13. Sample Cu 3. Difference ΔS between the thermoelectric power of a copper foil of thickness $a_1 = 5.08 \times 10^{-3}$ mm and a copper wire of diameter $a_2 = 0.254$ mm as a function of temperature. ($RR_{wire} = 1538$ and $RR_{foil} = 91$)

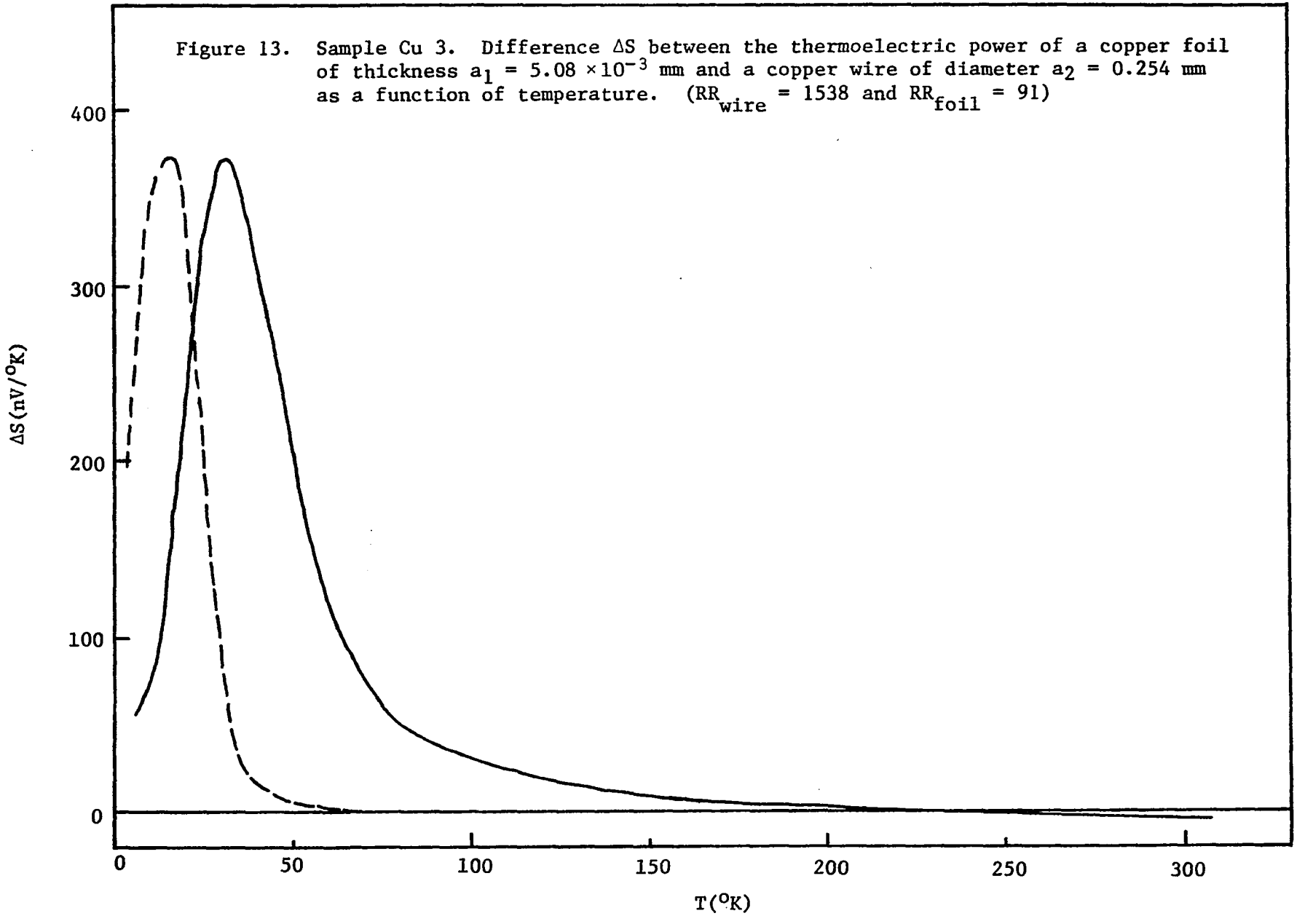

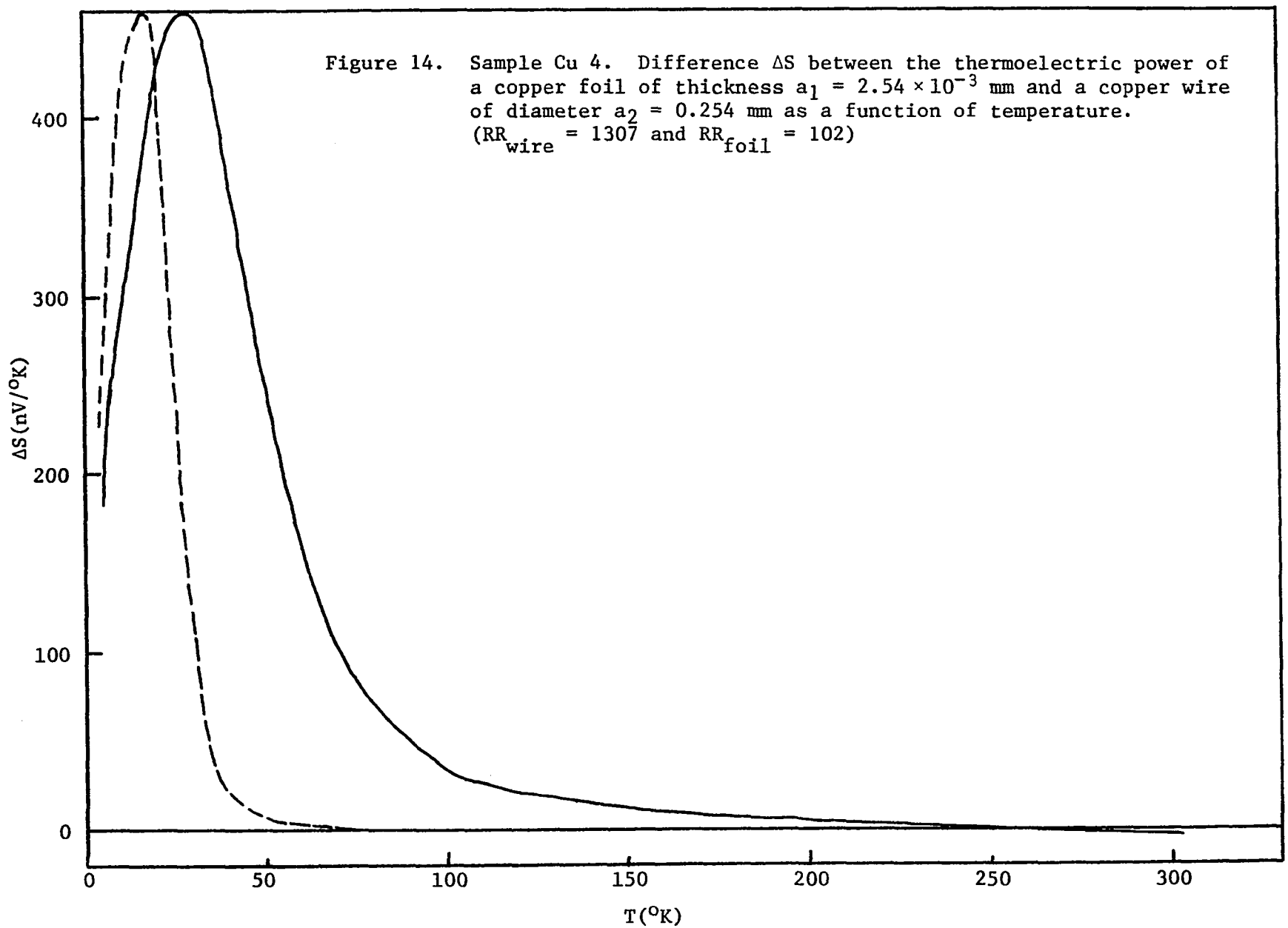

Figure 14. Sample Cu 4. Difference ΔS between the thermoelectric power of a copper foil of thickness $a_1 = 2.54 \times 10^{-3}$ mm and a copper wire of diameter $a_2 = 0.254$ mm as a function of temperature. ($RR_{wire} = 1307$ and $RR_{foil} = 102$)

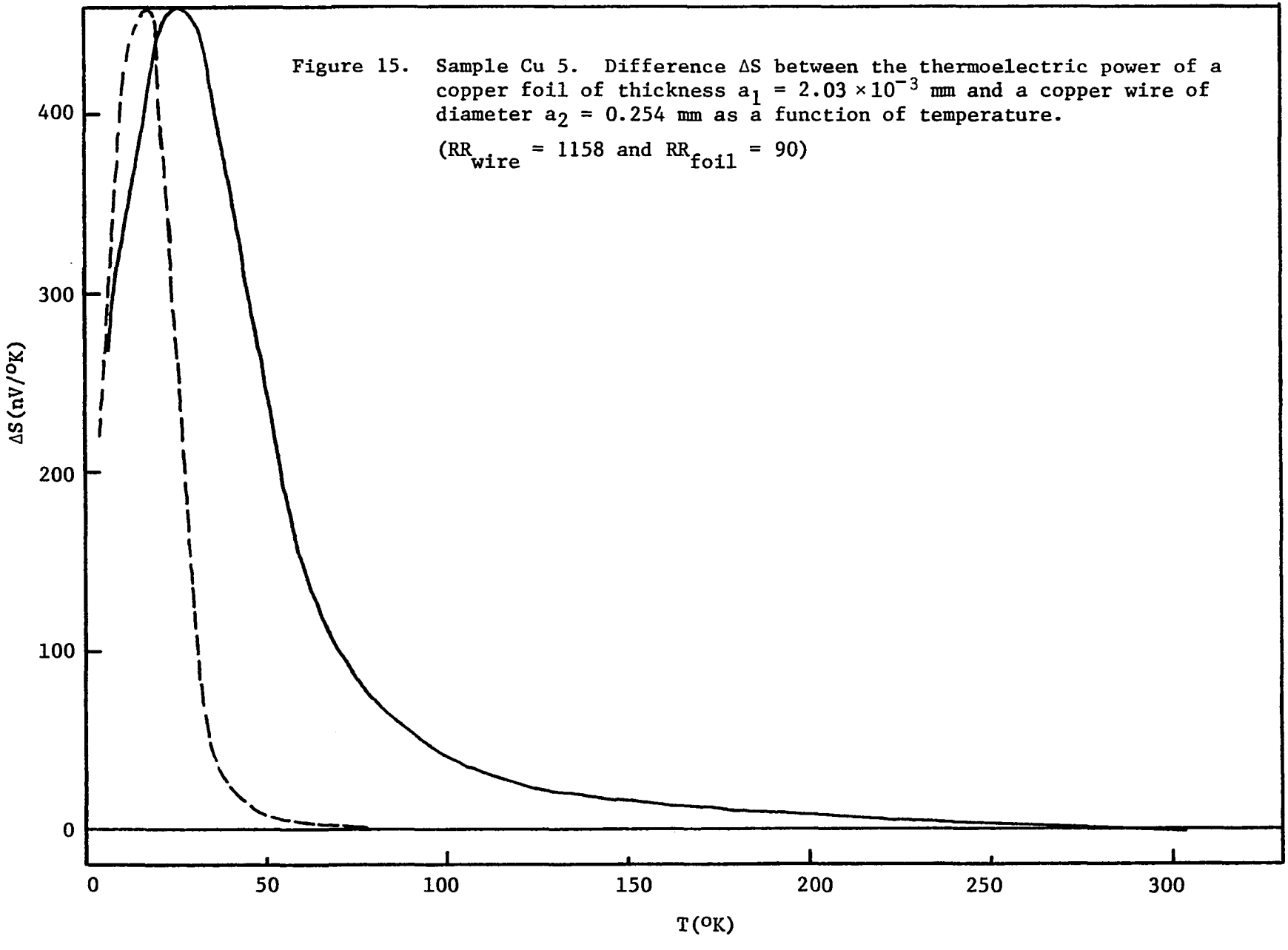

Figure 15. Sample Cu 5. Difference ΔS between the thermoelectric power of a copper foil of thickness $a_1 = 2.03 \times 10^{-3}$ mm and a copper wire of diameter $a_2 = 0.254$ mm as a function of temperature.

($RR_{wire} = 1158$ and $RR_{foil} = 90$)

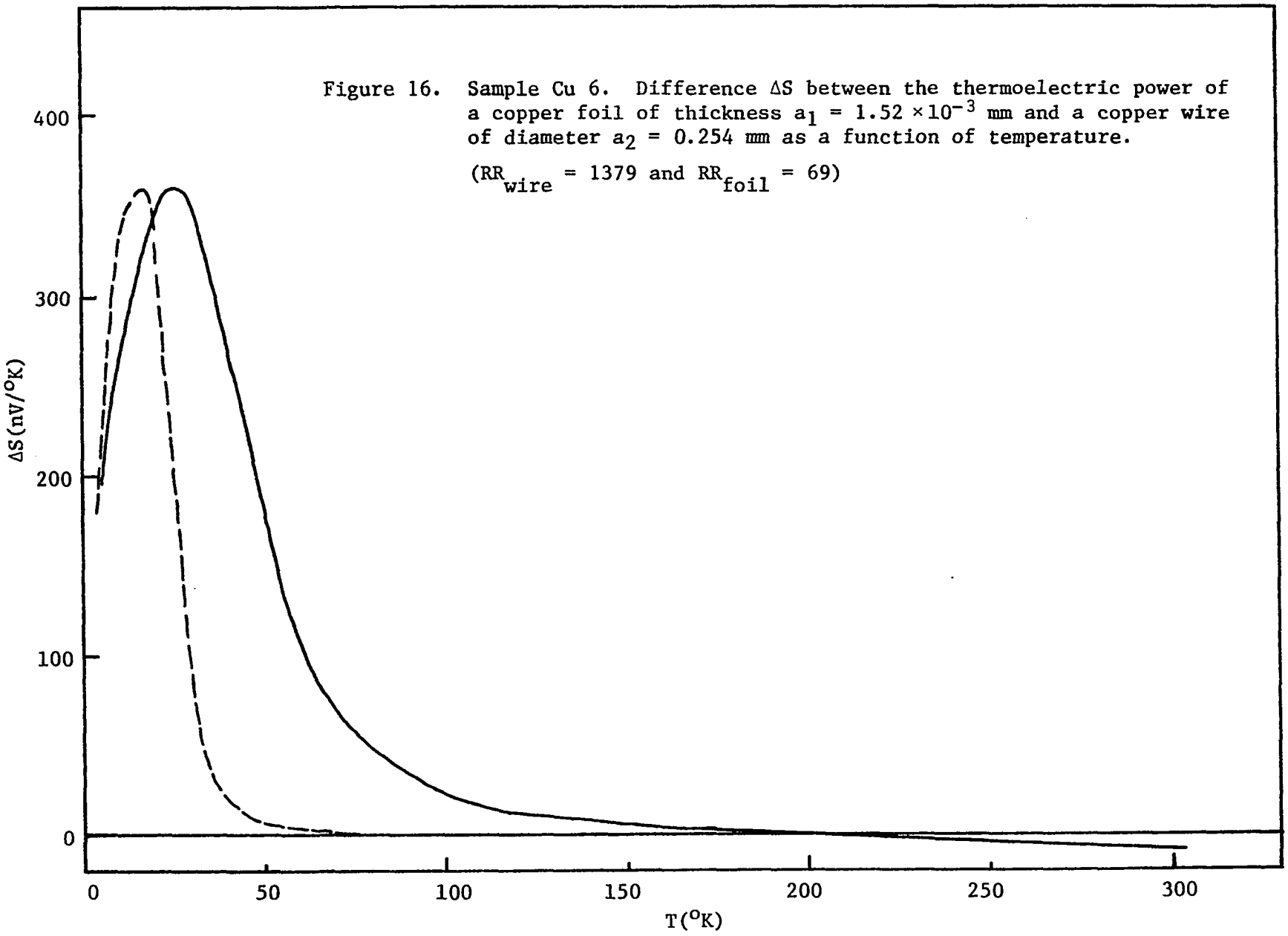

Figure 16. Sample Cu 6. Difference ΔS between the thermoelectric power of a copper foil of thickness $a_1 = 1.52 \times 10^{-3}$ mm and a copper wire of diameter $a_2 = 0.254$ mm as a function of temperature.

($RR_{wire} = 1379$ and $RR_{foil} = 69$)

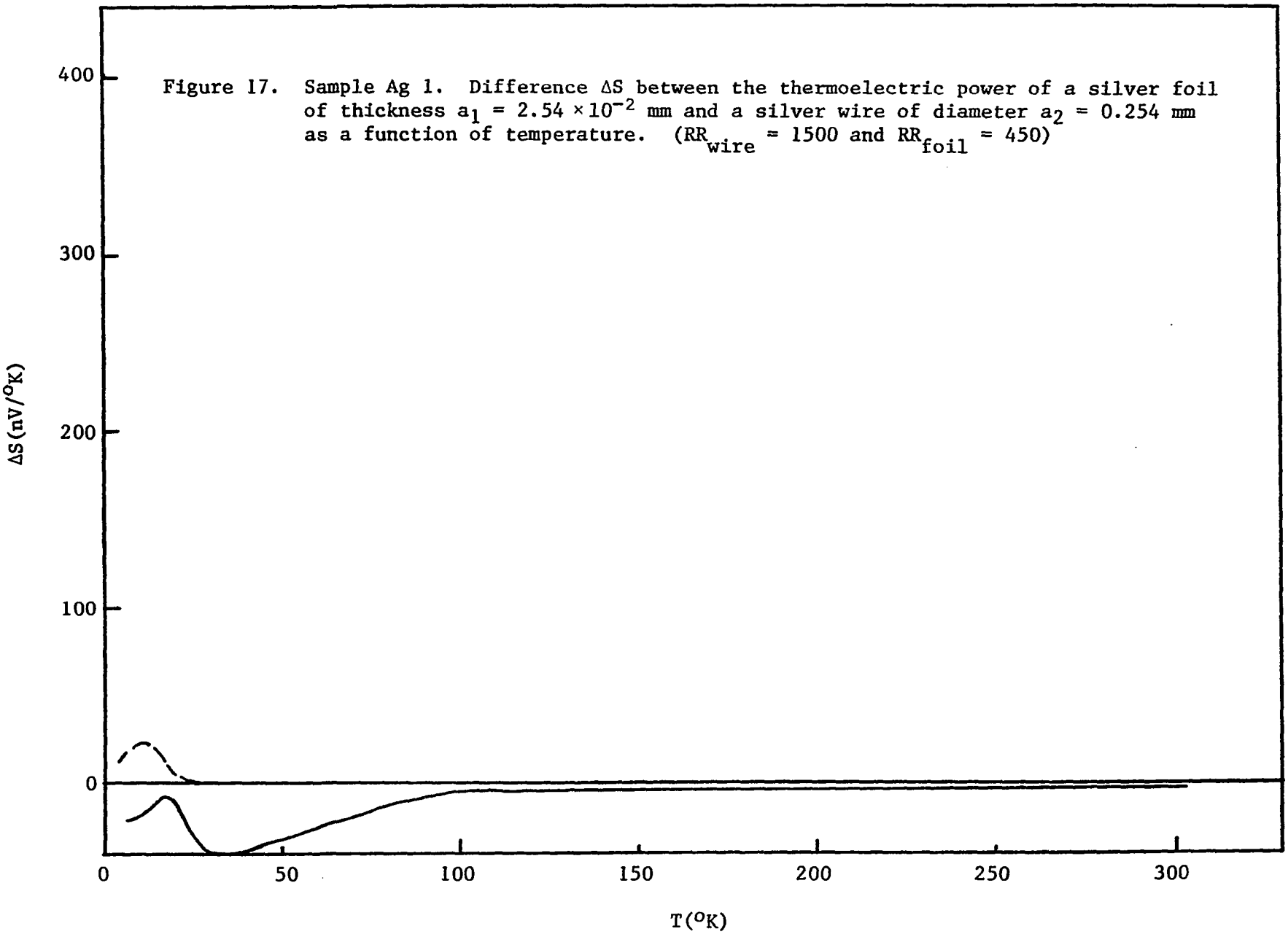

Figure 17. Sample Ag 1. Difference ΔS between the thermoelectric power of a silver foil of thickness $a_1 = 2.54 \times 10^{-2}$ mm and a silver wire of diameter $a_2 = 0.254$ mm as a function of temperature. ($RR_{wire} = 1500$ and $RR_{foil} = 450$)

Figure 18. Sample Ag 2. Difference ΔS between the thermoelectric power of a silver foil of thickness $a_1 = 1.27 \times 10^{-2}$ mm and a silver wire of diameter $a_2 = 0.254$ mm as a function of temperature. ($RR_{wire} = 1472$ and $RR_{foil} = 266$)

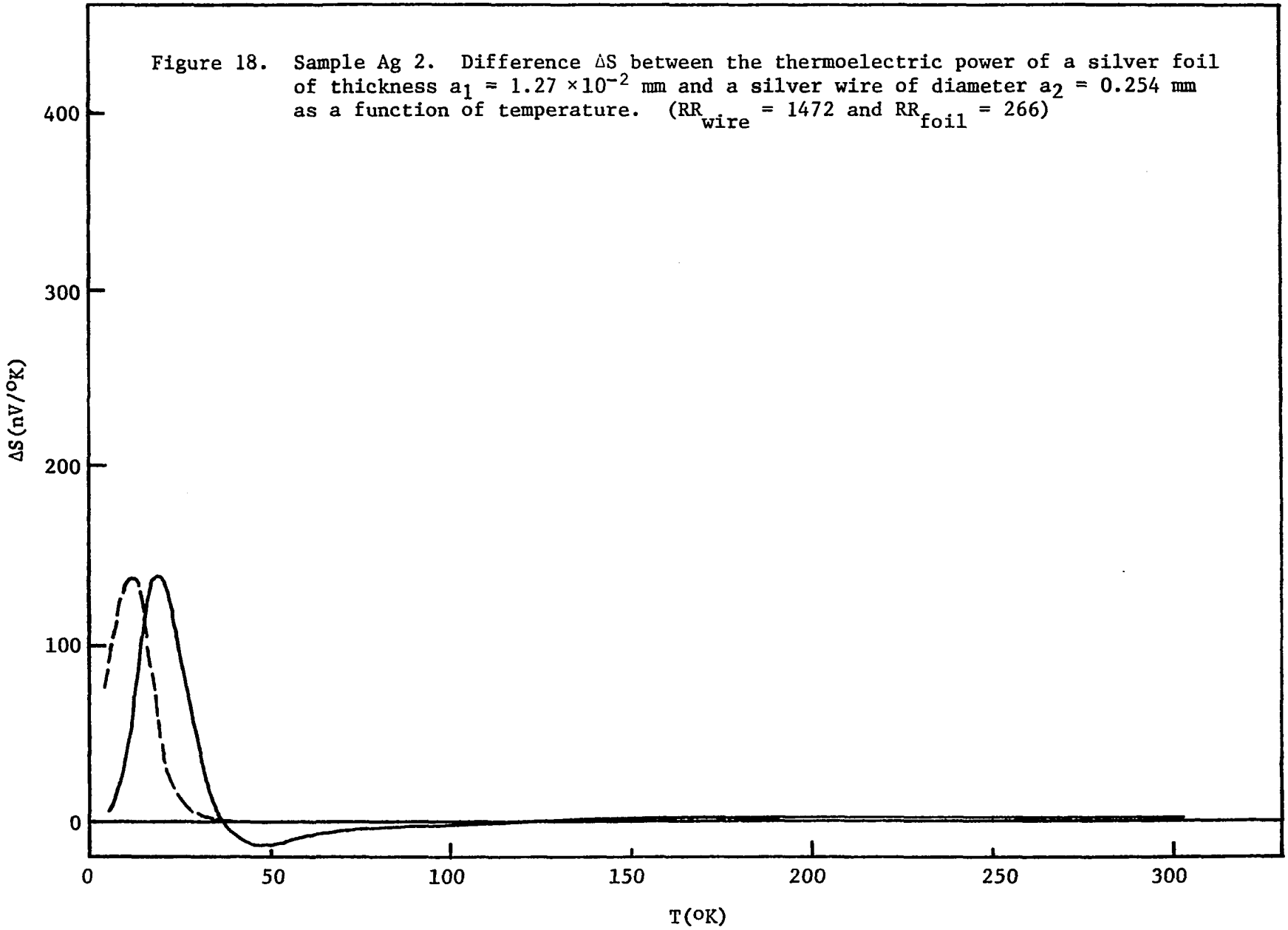

Figure 19. Sample Ag 3. Difference ΔS between the thermoelectric power of a silver foil of thickness $a_1 = 5.08 \times 10^{-3}$ mm and a silver wire of diameter $a_2 = 0.254$ mm as a function of temperature. ($RR_{wire} = 1525$ and $RR_{foil} = 158$)

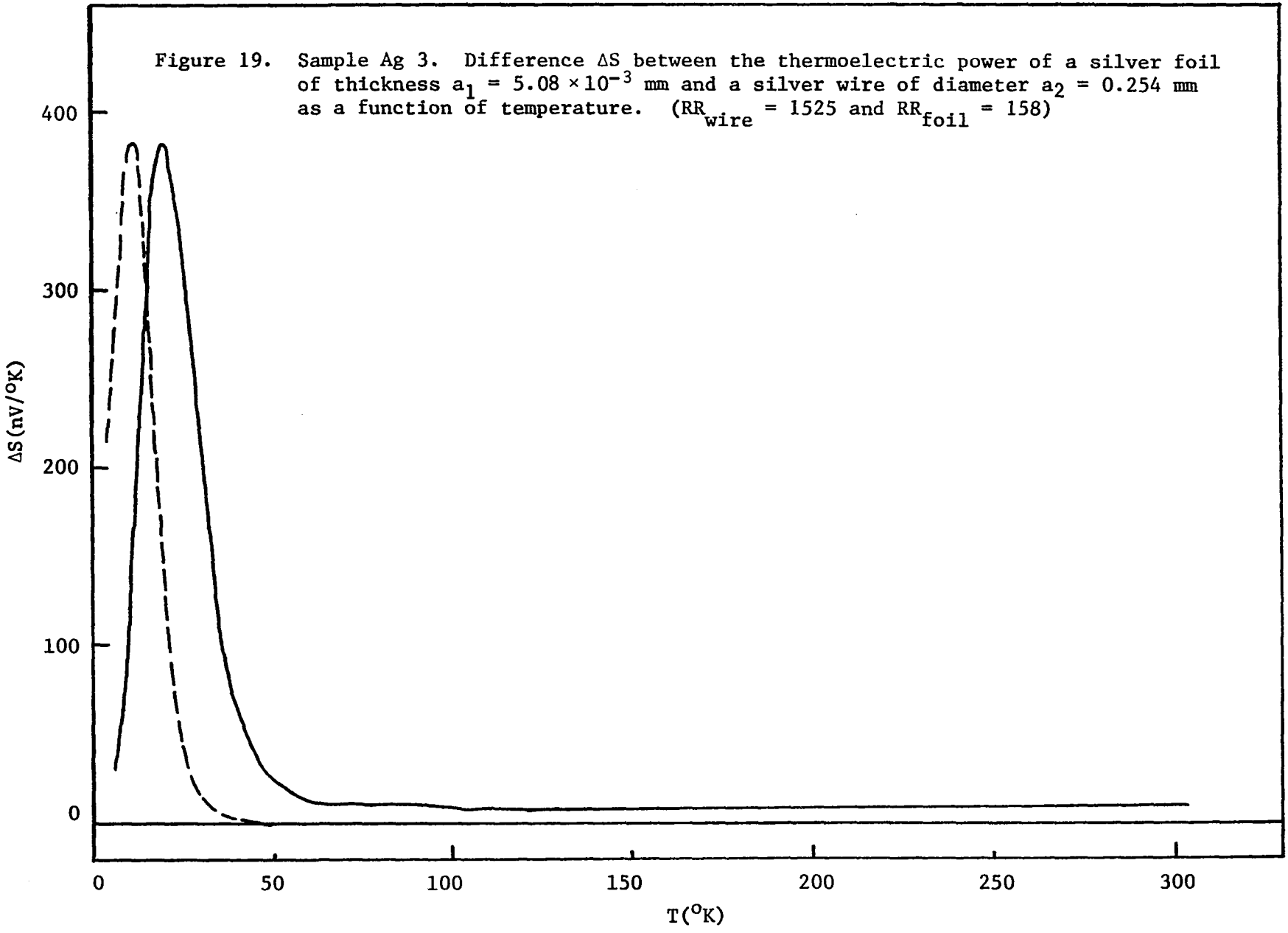

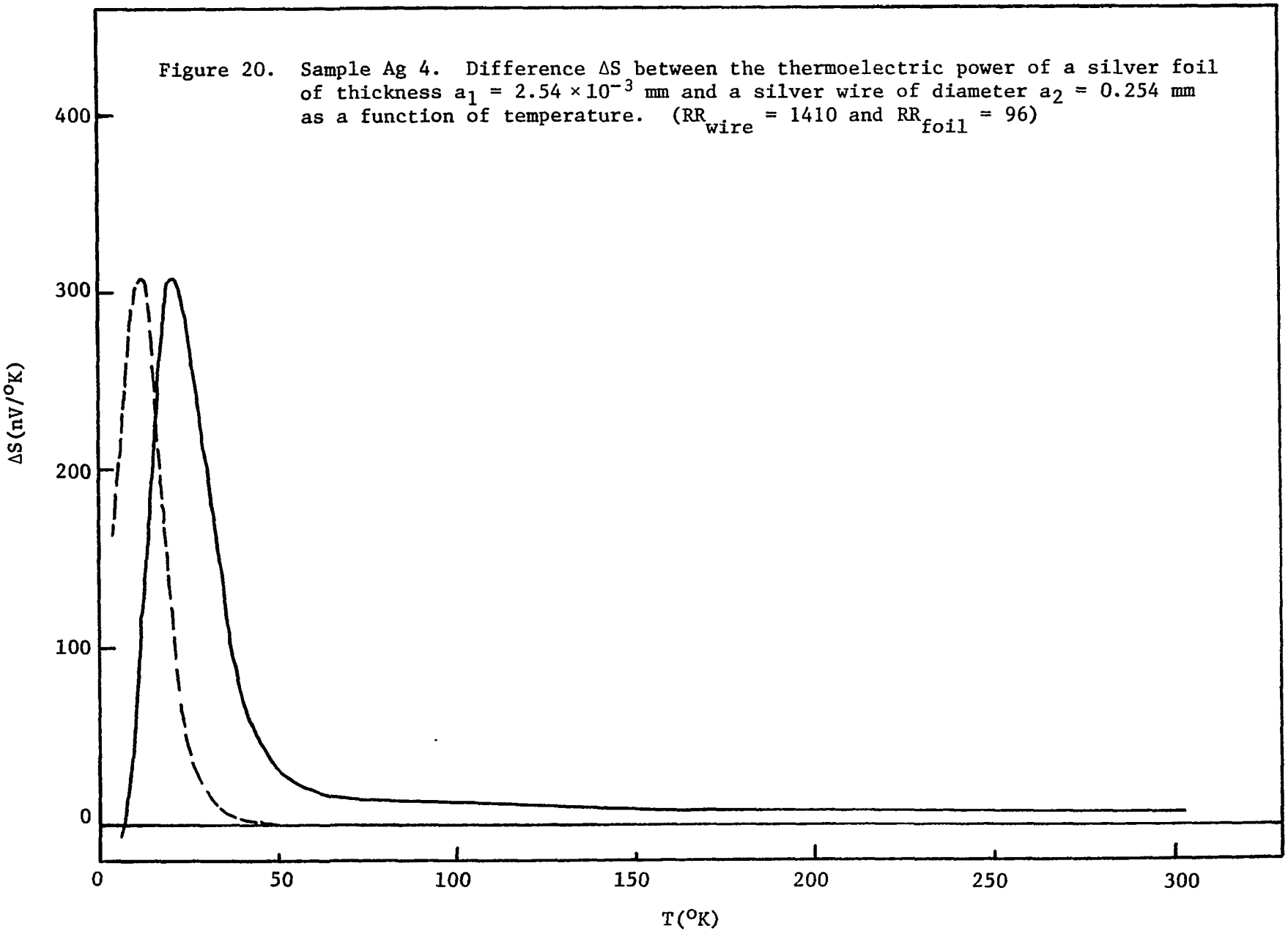

Figure 20. Sample Ag 4. Difference ΔS between the thermoelectric power of a silver foil of thickness $a_1 = 2.54 \times 10^{-3}$ mm and a silver wire of diameter $a_2 = 0.254$ mm as a function of temperature. ($RR_{wire} = 1410$ and $RR_{foil} = 96$)

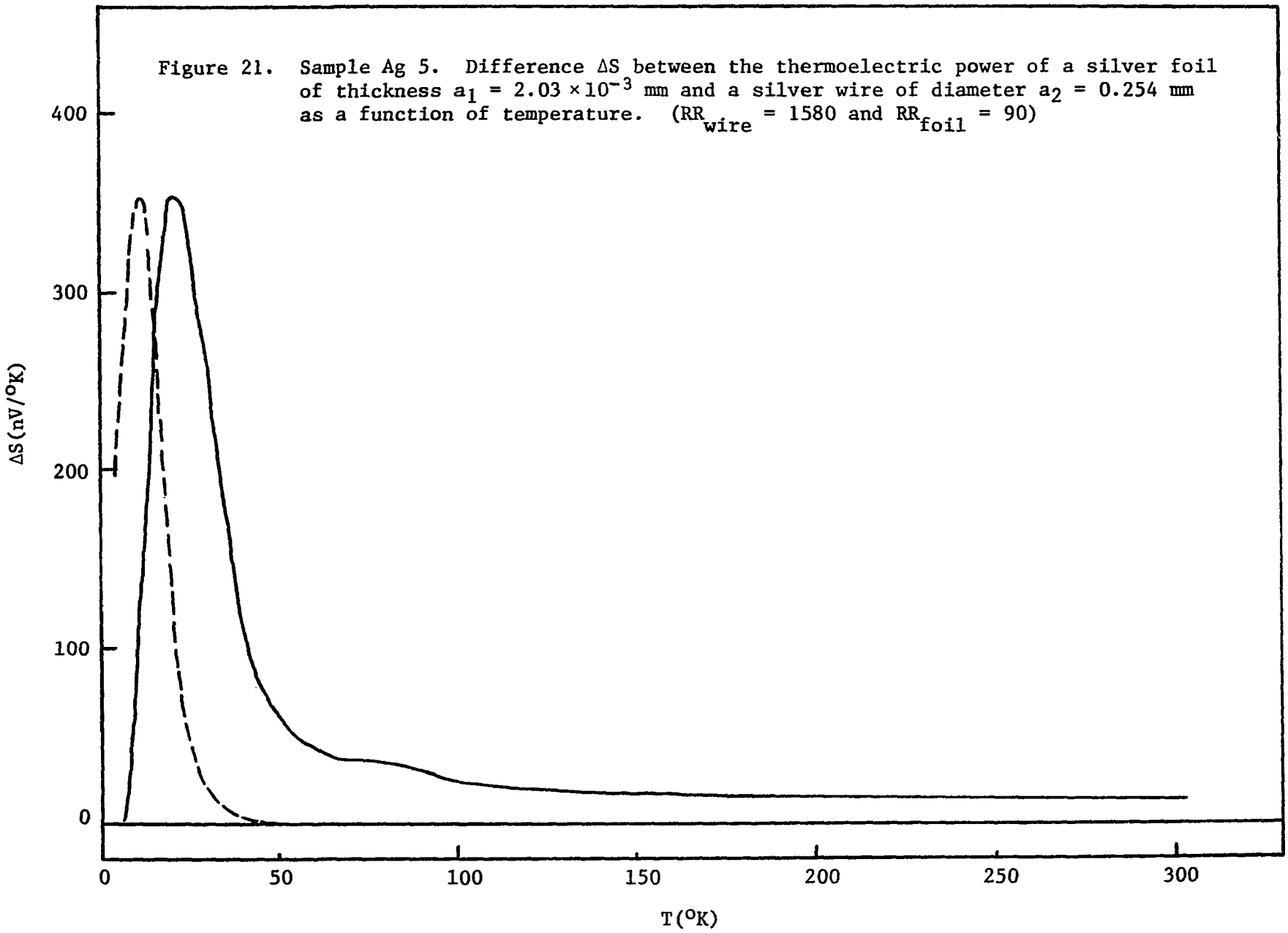

Figure 21. Sample Ag 5. Difference ΔS between the thermoelectric power of a silver foil of thickness $a_1 = 2.03 \times 10^{-3}$ mm and a silver wire of diameter $a_2 = 0.254$ mm as a function of temperature. ($RR_{wire} = 1580$ and $RR_{foil} = 90$)

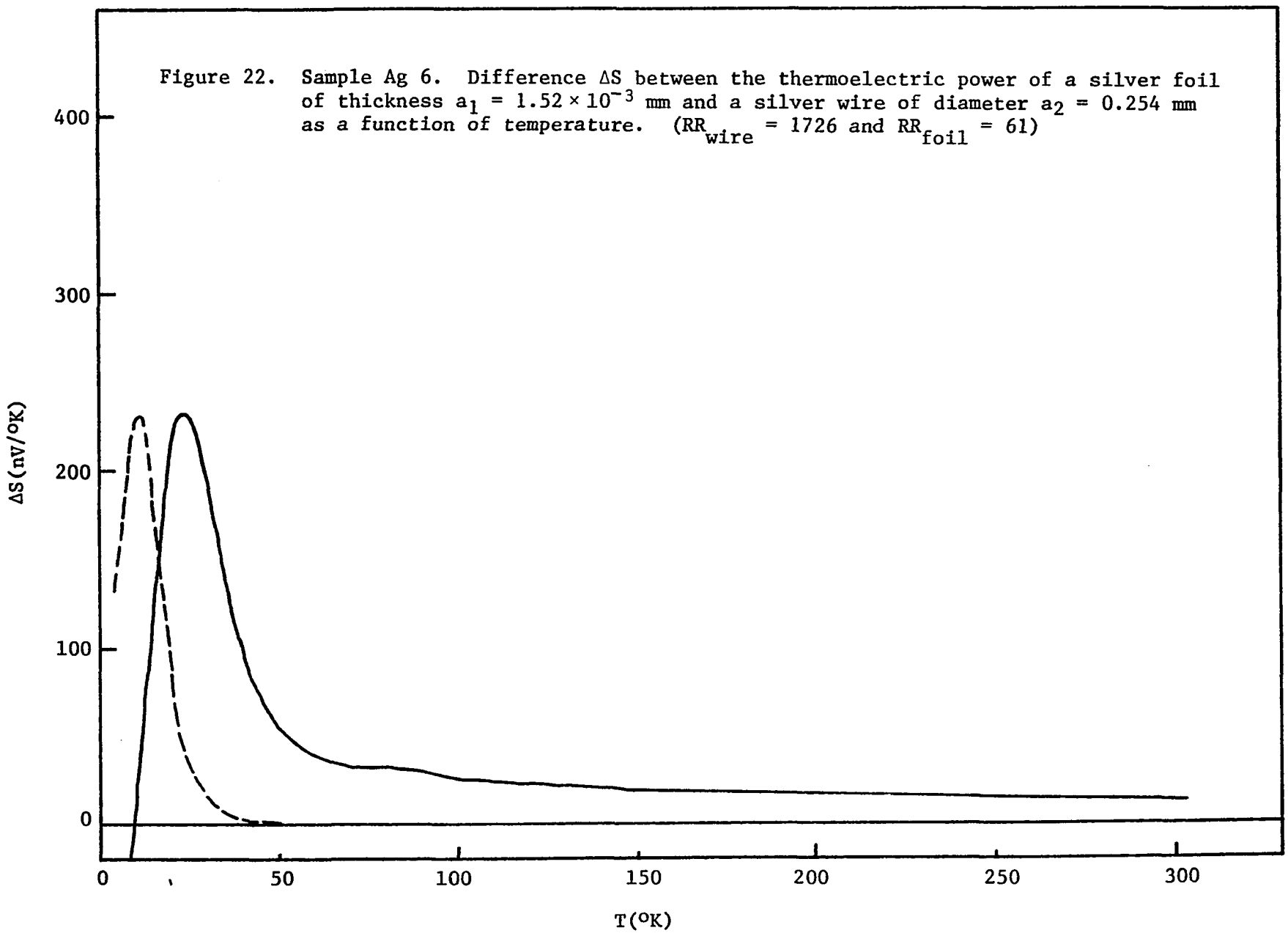

Figure 22. Sample Ag 6. Difference ΔS between the thermoelectric power of a silver foil of thickness $a_1 = 1.52 \times 10^{-3}$ mm and a silver wire of diameter $a_2 = 0.254$ mm as a function of temperature. ($RR_{wire} = 1726$ and $RR_{foil} = 61$)

The resistance ratio (RR) for well-annealed foils was measured to be between 77 and 442 for gold, between 60 and 558 for copper, and between 61 and 450 for silver. For well-annealed wires the resistance ratio (RR) was measured to be between 1074 and 1683 for gold, between 1109 and 1538 for copper, and between 1410 and 1726 for silver.

Analysis of High Temperature Results

The high temperature results were analyzed by the techniques developed by Huebener for gold[10] and platinum[18].

The difference in the electrical resistivity of the foils and the 0.254 mm wires was determined from their resistance at 296 ^{o}K to that at 77.3 ^{o}K and at 4.2 ^{o}K. With

$$\{\rho(296\ ^{o}K)/\rho(T')\}_{foil} \equiv A \qquad (51)$$

and

$$\{\rho(296\ ^{o}K)/\rho(T')\}_{wire} \equiv B \qquad (52)$$

the resistivity $\Delta\rho$ between a foil and a wire is given by

$$\Delta\rho = \rho_{foil} - \rho_{wire} = \rho_{wire}(296\ ^{o}K)[(1-A/B)/(A-1)] , \qquad (53)$$

assuming that $\Delta\rho$ is independent of temperature. Here T' is either 77.3 ^{o}K or 4.2 ^{o}K. From Eq. (19) we know that

$$\Delta\rho = \frac{3}{4}\left(\frac{1}{2a_1} - \frac{1}{a_2}\right)\rho_o \ell , \qquad (54)$$

for the difference in the electrical resistivity of a foil of thickness a_1 and a wire of diameter a_2.

The resistivity difference $\Delta\rho$ was calculated for the various foil sizes in gold, copper and silver with Eq. (53). This is shown in Figs. 23-25 for $T' = 77.3\ ^{o}K$ and $T' = 4.2\ ^{o}K$ as a function of the geometric quantity $(1/2a_1 - 1/a_2)$. In the calculations of $\Delta\rho$ the values

$$\rho_{wire}(296\ ^{o}K) = 22.25 \times 10^{-7}\ \Omega\,cm \tag{55}$$

$$\rho_{wire}(296\ ^{o}K) = 17.24 \times 10^{-7}\ \Omega\,cm \tag{56}$$

$$\rho_{wire}(296\ ^{o}K) = 15.9 \times 10^{-7}\ \Omega\,cm \tag{57}$$

were used for gold, copper, and silver respectively. As seen in Figs. 23-25 $\Delta\rho$ increases linearly with $(1/2a_1 - 1/a_2)$. From Figs. 23-25 and Eq. (54) we find

$$\ell\rho_o = (19.64 \pm 1.97) \times 10^{-12}\ \Omega\,cm^2 \tag{58}$$

$$\ell\rho_o = (14.25 \pm 0.35) \times 10^{-12}\ \Omega\,cm^2 \tag{59}$$

$$\ell\rho_o = (9.386 \pm 0.95) \times 10^{-12}\ \ cm^2 \tag{60}$$

for gold, copper, and silver respectively. With the values of $\rho_o(296\ ^{o}K) \simeq \rho_{wire}(296\ ^{o}K)$ given in Eqs. (55)-(57) we then obtain

$$\ell T = (2.61 \pm 0.26) \times 10^{-3}\ cm\ ^{o}K \tag{61}$$

for gold,

$$\ell T = (2.45 \pm 0.06) \times 10^{-3}\ cm\ ^{o}K \tag{62}$$

for copper, and

$$\ell T = (1.75 \pm 0.18) \times 10^{-3}\ cm\ ^{o}K \tag{63}$$

for silver in the temperature range in which ρ_{wire} is linearly proportional to the temperature.

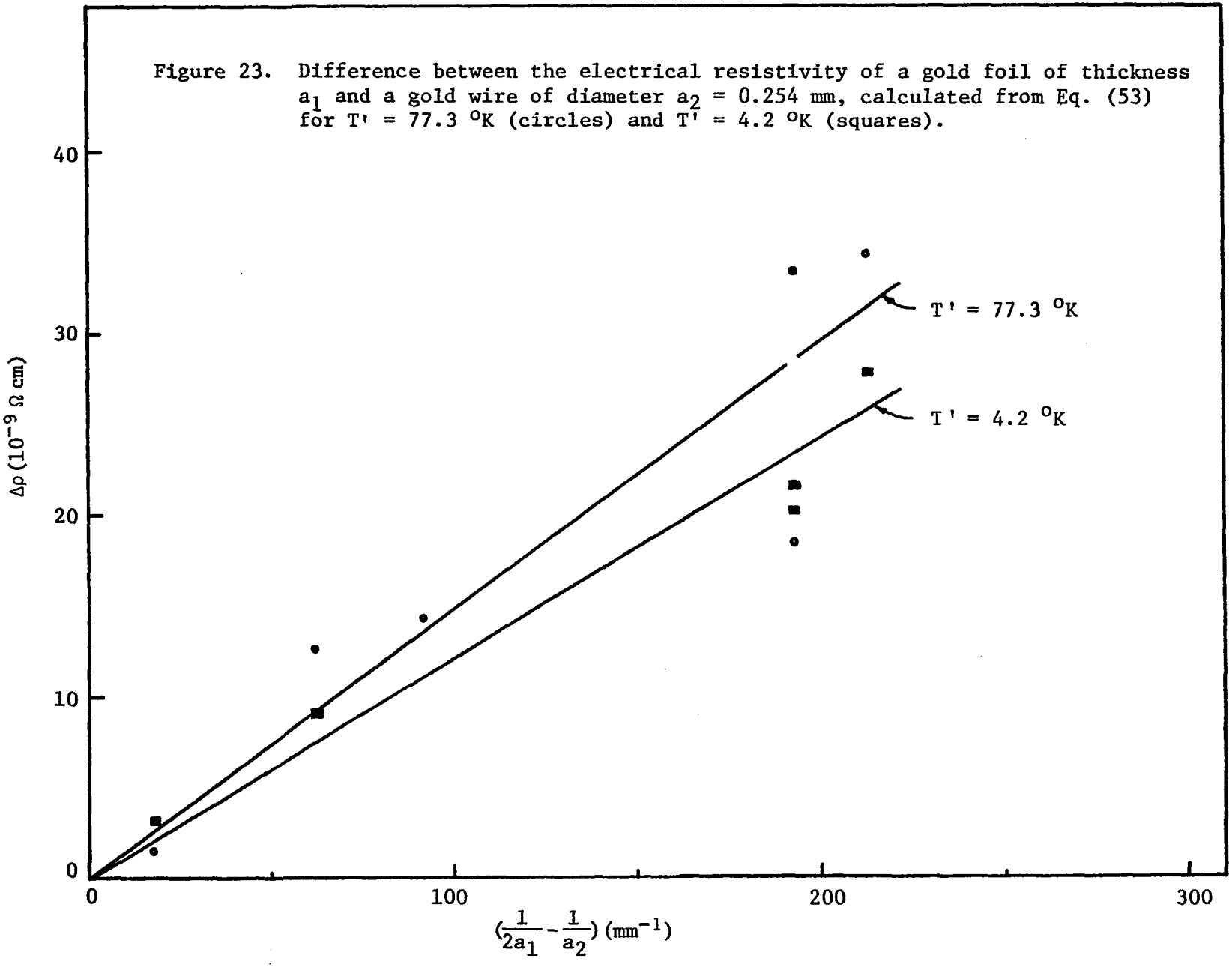

Figure 23. Difference between the electrical resistivity of a gold foil of thickness a_1 and a gold wire of diameter a_2 = 0.254 mm, calculated from Eq. (53) for T' = 77.3 °K (circles) and T' = 4.2 °K (squares).

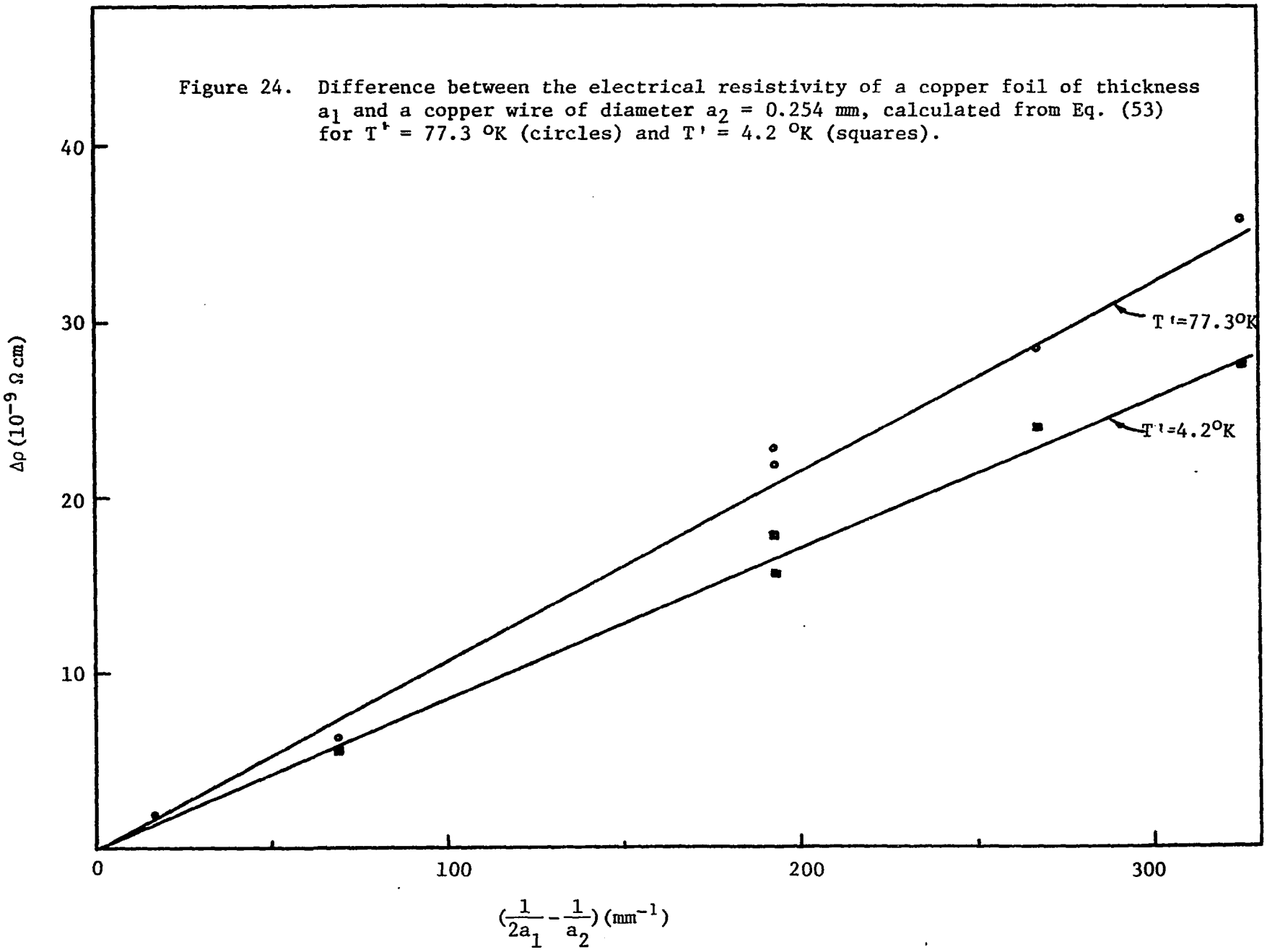

Figure 24. Difference between the electrical resistivity of a copper foil of thickness a_1 and a copper wire of diameter a_2 = 0.254 mm, calculated from Eq. (53) for $T' = 77.3\ ^{o}K$ (circles) and $T' = 4.2\ ^{o}K$ (squares).

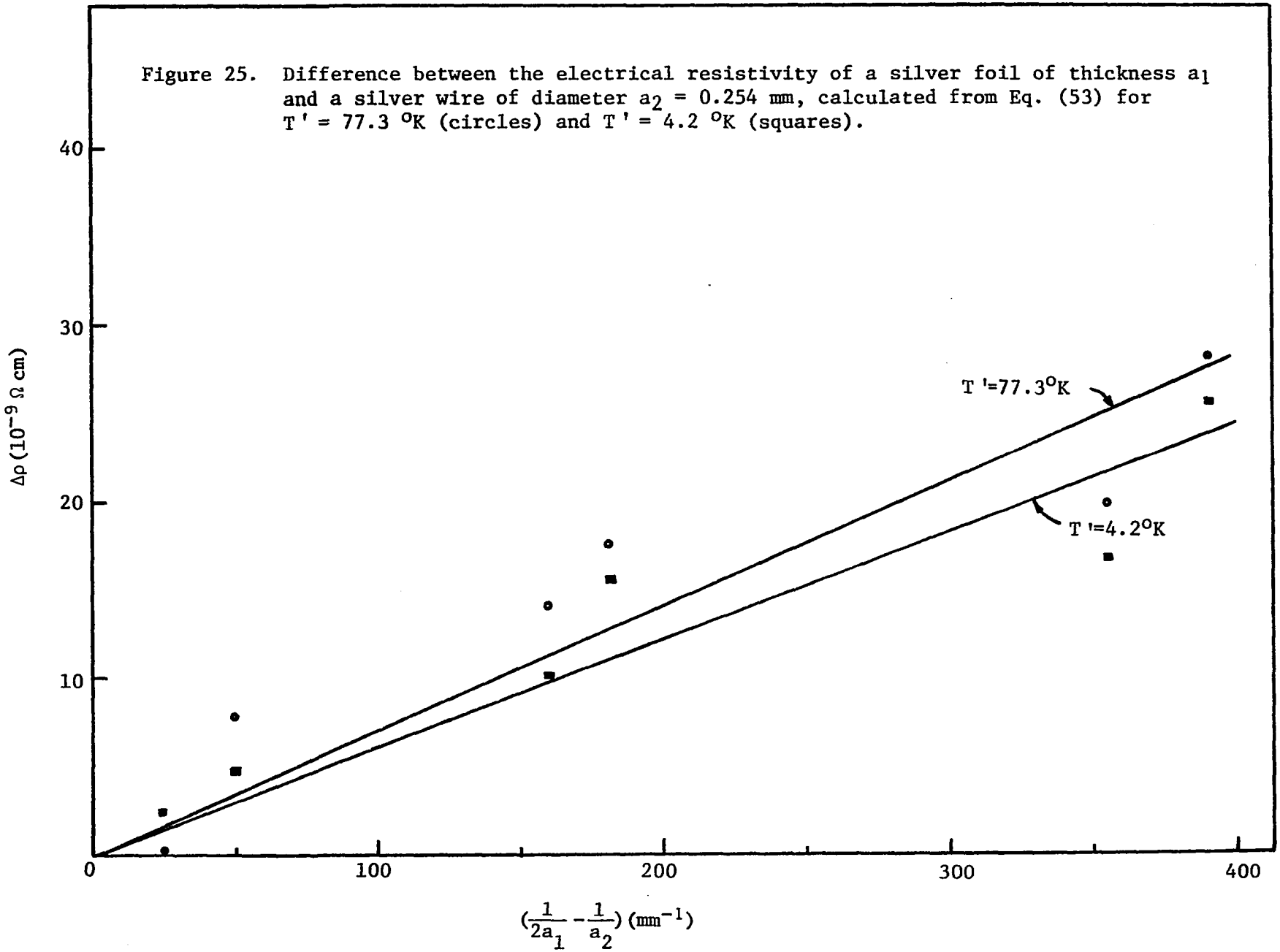

Figure 25. Difference between the electrical resistivity of a silver foil of thickness a_1 and a silver wire of diameter a_2 = 0.254 mm, calculated from Eq. (53) for T ' = 77.3 °K (circles) and T ' = 4.2 °K (squares).

Figure 26 shows the average change in the electronic thermoelectric power of a thermocouple consisting of a foil and a wire as a function of the geometric quantity $(1/2a_1-1/a_2)$. The points for Fig. 26 were obtained by averaging the thermoelectric power values for each foil in the region where the thermoelectric power curves were constant. In this region the phonon-drag contribution is negligible. For gold this is good for T>100 ^{o}K, for copper T 250 ^{o}K, and for silver for T>100 ^{o}K. To check the values of $\overline{\Delta S_e}$ plotted in Fig. 26 an average measurement of ΔS_e between 77.3 ^{o}K and 296 ^{o}K was performed in the same manner as Huebener for gold[10]. This was only possible for gold and silver, but the results in these two cases agreed with our point by point measurements to within 16 per cent. Since increasing foil and wire size imply no size effect, the points in Fig. 26 were fitted to a straight line through the origin for each of the noble metals. With Eq. (23) and the results of Fig. 26 the values of $\{\partial \ell n \ell(\varepsilon)/\partial \ell n \varepsilon\}_{\varepsilon_F} = U$ were calculated. These values are given in Table 1. In these calculations the average values of ℓT given in Eqs. (61) to (63), $\varepsilon_F(Au) = 5.51$ eV, $\varepsilon_F(Cu) = 7.0$ eV, and $\varepsilon_F(Ag) = 5.5$ eV were used. The values of U given in Table 1 are, of course, an average value over the Fermi surface. With the values of U, Eq. (15), and the values

$$\frac{S_e^o}{T} = 7.05 \times 10^{-3} \mu V/^{o}K^2 \qquad (64)$$

for gold[42],

$$\frac{S_e^o}{T} = 5.4 \times 10^{-3} \ \mu V/^{o}K^2 \qquad (65)$$

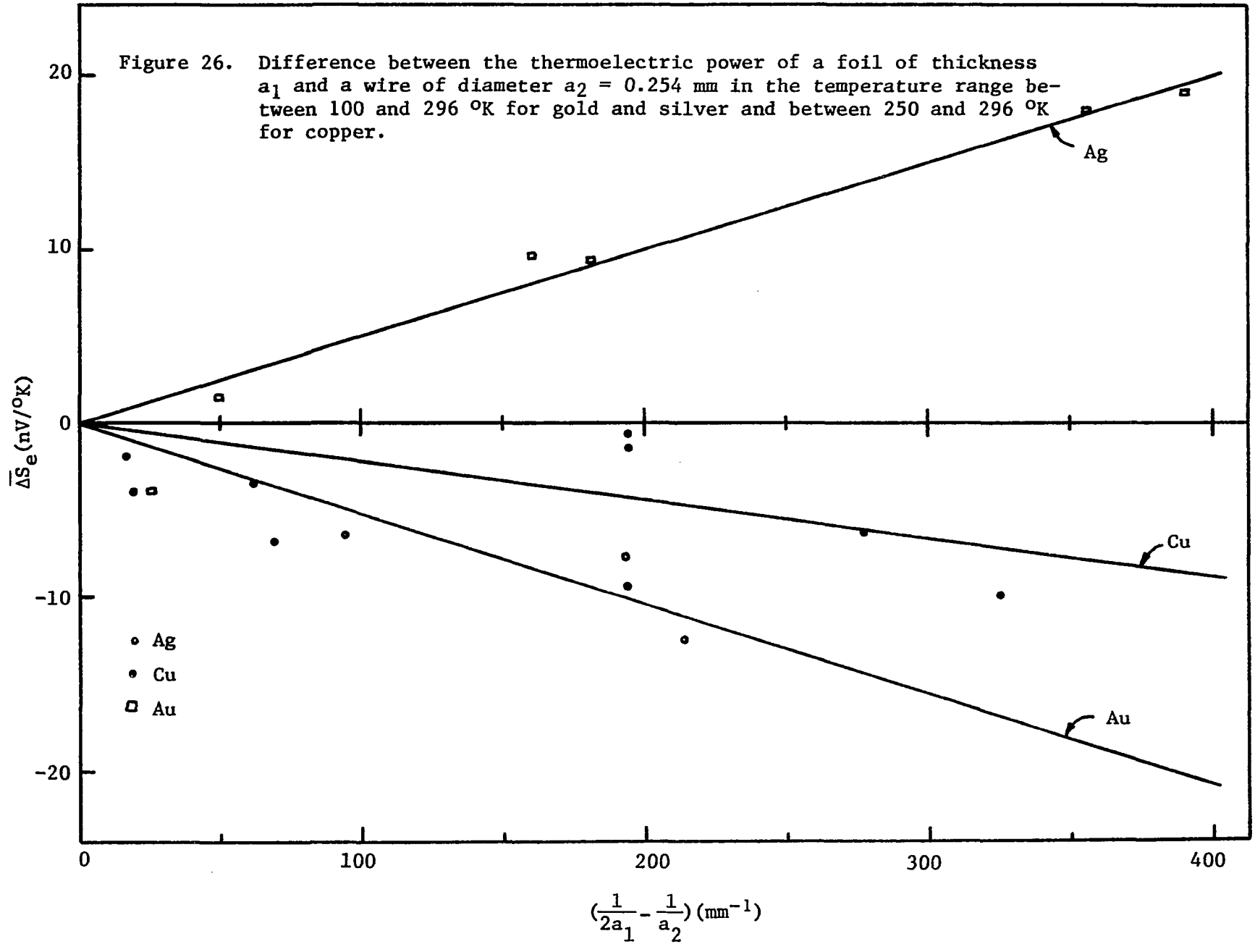

Figure 26. Difference between the thermoelectric power of a foil of thickness a_1 and a wire of diameter a_2 = 0.254 mm in the temperature range between 100 and 296 °K for gold and silver and between 250 and 296 °K for copper.

Table 1. High Temperature Results $\left\{\frac{\partial \ell n \ell(\varepsilon)}{\partial \ell n \varepsilon}\right\}_{\varepsilon_F}$

	This Experiment	Huebener[10]	Lin and Leonard[23]	Worobey *et al.*[24]	Angus and Dalgliesh[22]	Gouault[19]
Au	-0.58±0.08	-0.53±0.19	-0.60±0.04	-0.61±0.20	+0.9	-
Cu	-0.34±0.11	-	-	-	+2.3	+2.1
Ag	+0.86±0.09	-	-	-	+2.7	-

$\left\{\frac{\partial \ell n A(\varepsilon)}{\partial \ell n \varepsilon}\right\}_{\varepsilon_F}$

	This Experiment	Huebener[10]	Lin and Leonard[23]	Worobey[24]	Angus and Dalgliesh[22]	Gouault[19]
Au	-1.00±0.08	-1.05±0.19	-0.85±0.04	-0.98±0.20	-2.5	-
Cu	-1.20±0.11	-	-	-	-3.8	-3.6
Ag	-1.91±0.09	-	-	-	-3.8	-

for copper[26], and

$$\frac{S_e^o}{T} = 4.7 \times 10^{-3} \ \mu V/^oK \qquad (66)$$

for silver[55], we obtain the values of V for the noble metals given in Table 1. Along with the values for U and V calculated in this experiment, the other published values for these quantities are included in Table 1 for comparison.

Analysis of Low Temperature Results

In Eq. (34) we have expressed the change in the electronic thermoelectric power due to magnetic impurities as

$$\Delta S = \rho_3 S_o \frac{T}{T+T_o} \left(\frac{1}{\rho^f} - \frac{1}{\rho^w}\right) \ , \qquad (67)$$

where $\rho^{f,w} = \rho_o^{f,w} + \Delta\rho^{f,w}$. The change in the resistivity $\Delta\rho$ was obtained from the resistance ratio of each foil or wire and $\rho(296\ ^oK)$ for each of the noble metals. ΔS was then calculated from Eq. (67) and fitted to the experimental curves given in Figs. 5-22 giving the dashed curves in Figs. 5-22.

The product $\rho_3 S_o$ was used as a fitting parameter to adjust the height of peak to that of the experimental peak. The values of T_o for gold and copper were taken from Daybell and Steyert[56] as

$$T_o = 9\ ^oK \qquad (68)$$

for gold, and

$$T_o = 30\ ^oK \qquad (69)$$

for copper. For silver T_o was also used as a fitting parameter to

adjust the peak position. As T_o increases, the calculated peak position becomes fixed due to the rapid fall off of $(1/\rho^f - 1/\rho^w)$ [see Eq. (67)]. Thus, T_o could not be determined uniquely in this way. The calculated peak position for silver did not change significantly for T_o values higher than 25 ^oK, so we chose to use the value of T_o in silver as

$$T_o = 25\ ^oK\ . \tag{70}$$

The values obtained for the product $\rho_3 S_o$ are given in Table 2. The interpretation of these values can be carried out in two ways. We can either assume a value for S_o and determine ρ_3 or assume a value for ρ_3 and calculated S_o. In either case we are able to estimate the concentration of unoxydized iron present.

Method I: First let us assume that we know S_o. Values of S_o at low temperatures have been reported as

$$S_o = -14.7\ \mu V/^oK \tag{71}$$

for gold[34],

$$S_o = -16.0\ \mu V/^oK \tag{72}$$

for copper[26], and

$$S_o = -7.5\ \mu V/^oK \tag{73}$$

for silver[27]. We should note at this point that the form $S_o T/(T+T_o)$ is well established for low temperatures (below 10 ^oK) but, until this experiment, could not be investigated at higher temperatures because the effect of magnetic impurities is normally masked by the pure metal thermoelectric power above 10 ^oK.

Table 2. Values of Low Temperature Fitting Parameter $\rho_3 S_o$.

Sample Number (Au,Cu,Ag)	$\rho_3 S_o$(Au) (10^{-8} Ω cm V/°K)	$\rho_3 S_o$(Cu) (10^{-8} Ω cm V/°K)	$\rho_3 S_o$(Ag) (10^{-8} Ω cm V/°K)
1	-0.157	-0.205	-0.015
2	-0.234	-0.193	-0.074
3	-0.217	-0.199	-0.178
4	-0.137	-0.278	-0.145
5	-0.130	-0.301	-0.151
6	-0.109	-0.202	-0.090

Theoretically[56], it is expected that S_o would decrease with increasing temperature, so we expect the values given for S_o in Eqs. (71) to (73) to be upper limits and the concentrations determined with them to be lower limits. With the values of S_o in Eqs. (71) to (73) we can obtain values of ρ_3 which are given in Table 3. For very dilute alloys (less than 100 ppm) the resistivity of the iron present can be assumed to be proportional to the concentration of unoxydized iron present in the sample. Values of the constants of proportionality were taken as

$$\alpha = 1.3 \times 10^{-3} \frac{\mu\,\Omega\,cm}{ppm} \tag{74}$$

for gold[28],

$$\alpha = 1.0 \times 10^{-3} \frac{\mu\,\Omega\,cm}{ppm} \tag{75}$$

for copper[55], and

$$\alpha = 0.8 \times 10^{-3} \frac{\mu\,\Omega\,cm}{ppm} \tag{76}$$

for silver[29]. Thus, we are able to estimate the concentration of unoxydized magnetic impurity in each of the samples. These are given in Table 3.

Method II: We now consider a second method to determine the resistivity and concentration of unoxydized iron. Using the values of $\rho_3 S_o$ in Table 2 we can then determine new values of S_o.

The measured values of the resistivities of the wires at 4.2 ^oK are made up of size effects; ρ_{SE}, unoxydized iron impurities, ρ_3^{new}, and other (non-magnetic) impurities, $\Delta\rho_o$. That is,

$$\rho_{wire} = \rho_{SE} + \rho_3^{new} + \Delta\rho_o \quad . \tag{77}$$

Table 3. Method I: Values of Iron Resistivity and Concentration

Sample Number (Au,Cu,Ag)	ρ_3(Au) ($10^{-4}\mu\Omega$cm)	Concentration (ppm)	ρ_3(Cu) ($10^{-4}\mu\Omega$cm)	Concentration (ppm)	ρ_3(Ag) ($10^{-4}\mu\Omega$cm)	Concentration (ppm)
1	1.068	0.08	1.281	0.13	.201	0.02
2	1.592	0.12	1.206	0.12	.980	0.12
3	1.476	0.11	1.244	0.12	2.373	0.30
4	0.932	0.07	1.738	0.17	1.933	0.24
5	0.884	0.07	1.881	0.19	2.013	0.25
6	0.741	0.06	1.262	0.13	1.201	0.15

If we correct for size effects using Eqs. (17) and (18), we can write

$$\rho'_{wire} \equiv \rho_{wire} - \rho_{SE} = \rho_3^{new} + \Delta\rho_o \quad . \tag{78}$$

Now the non-magnetic impurities are assumed not to be effected by oxygen annealing, and since each sample of a given material came from the same spool of wire, $\Delta\rho_o$ is a constant for each material.

Also, we know that ρ_3^{new} is proportional to the experimentally determined product $\rho_3 S_o$. Then,

$$\rho'_{wire} = B(\rho_3 S_o) + \Delta\rho_o \quad . \tag{79}$$

By plotting ρ'_{wire} versus $\rho_3 S_o$ we determine B and $\Delta\rho_o$. The value of $\Delta\rho_o$ is then used in Eq. (78) to determine ρ_3^{new} Then using

$$S_o^{new} = \frac{\rho_3 S_o}{\rho_3^{new}} \quad , \tag{80}$$

we obtain new values for S_o.

The fact that the values of S_o^{new} are in all cases less than or equal to the low temperature values given in Eqs. (71) to (73) is consistent with our earlier assumption that these latter values are upper limits. The values of the concentrations of unoxydized iron present in the samples based on Method II are given along with S_o^{new} in Tables 4-6.

Table 4. Method II: Values of Parameters for Gold.

Sample Number (Au)	$\rho_w'(10^{-4}\mu\Omega cm)$ [ρ_w corrected for size effect]	ρ_3^{new} ($10^{-4}\,\mu\Omega\,cm$)	Concentration (ppm)	S_o^{new} ($\mu V/^oK$)
1	8.90	5.08	0.39	-3.1
2	11.0	7.58	0.58	-2.1
3	10.90	7.03	0.54	-2.2
4	8.90	4.44	0.34	-3.5
5	8.20	4.21	0.32	-3.7
6	7.02	3.53	0.27	-4.4

$B = -0.324\ ^oK/\mu V$ $\qquad$ $\Delta\rho_o = 3.83 \times 10^{-4}\,\mu\Omega\,cm$

Table 5. Method II: Values of Parameters for Copper

Sample Number (Cu)	$\rho'_w(10^{-4}\mu\Omega cm)$ [ρ_w corrected for size effect]	ρ_3^{new} $(10^{-4}\,\mu\Omega\,cm)$	Concentration (ppm)	S_o^{new} $(\mu V/^oK)$
1	5.57	2.78	0.28	-7.4
2	6.46	2.61	0.26	-7.4
3	5.22	2.70	0.27	-7.4
4	6.14	3.77	0.38	-7.4
5	6.93	4.08	0.41	-7.4
6	5.82	2.74	0.27	-7.4

$B = -0.136\ ^oK/\mu V$ $\qquad$ $\Delta\rho_o = 2.72\ \ 10^{-4}\,\mu\Omega\,cm$

Table 6. Method II: Values of Parameters for Silver

Sample Number (Ag)	$\rho_w'(10^{-4}\,\mu\Omega\,cm)$ [ρ_w corrected for size effect]	ρ_3^{new} $(10^{-4}\,\mu\Omega\,cm)$	Concentration (ppm)	S_o^{new} $(\mu V/^oK)$
1	9.07	.20	0.02	-7.5
2	9.24	.98	0.12	-7.5
3	8.92	2.37	0.30	-7.5
4	9.61	1.93	0.24	-7.5
5	8.61	2.01	0.25	-7.5
6	7.88	1.20	0.15	-7.5

$B = -0.133\ ^oK/\mu V$ $\qquad$ $\Delta\rho_o = 4.57 \times 10^{-4}\,\mu\Omega\,cm$

CHAPTER V

DISCUSSION AND CONCLUSIONS

High Temperature Results

The negative values of U given in Table 1 for gold and copper show the decrease in electron mean free path with increasing energy as suggested by Ziman[5], Blatt[7], and Robinson[9] and in strong disagreement with the free electron value of 2.0. The value of U for gold agrees well with the value obtained by Huebener[10], Lin and Leonard[23], and Worobey *et al.*[24] as seen in Table 1. The values of U for gold and copper agree in sign with Robinson's[9] theoretical estimates of -0.63 and -1.67 for gold and copper respectively. It has been suggested by Huebener[10] and Lin and Leonard[23] that the positive values of U obtained by Angus and Dalgliesh[22] and Gouault[19] were disturbed because the thin films could not be annealed at sufficiently high temperatures after deposition and as a result are probably masked by the presence of large concentrations of lattice defects within the films.

The values of V for gold and copper given in Table 1 are in agreement in that it is obvious that the area of Fermi surface decreases with increasing energy. This is in disagreement with Ziman's[5] value of 0.5 and Robinson's[10] assumption of the free electron value of 1.0.

It is concluded that for gold and copper that neither U nor V is separately responsible for the positive sign of the electronic thermoelectric power, but in fact both terms contribute.

A surprising result of this experiment is the positive value for U in the case of silver. While this agrees in sign with the value obtained by Angus and Dalgliesh[22] we have already noted that their results are in question. It also disagrees with Robinson's[9] theoretical estimate of -0.62. The positive value of U for silver shows that in this case the mean free path is increasing with increasing energy in disagreement with Ziman[5], Blatt[7], and Robinson[9]. The positive sign, in fact, is more characteristic of the free electron prediction. As in the case of gold and copper the value of V is negative, and in the case of silver, V is the dominant term giving rise to a positive electronic thermoelectric power.

It is apparent that Robinson's[9] theory does not explain the sign anomaly of the electronic thermoelectronic power in silver. In all of the noble metals existing theories are unable to explain the negative sign of V.

With the extremely accurate knowledge of the detailed shape of the Fermi surfaces of the noble metals now available from deHaas van Alphen studies, it would seem that a new theoretical calculation of the change in the area of the Fermi surface with energy, V, would be feasible and valuable to aid in clearing up the problem of the negative values of V found in this experiment. It is interesting that the problem of the positive sign of the absolute thermoelectric

power of the noble metals has been attacked by so many able theoretians for more than thirty five years and still lacks a complete explanation.

A successful experiment on evaporated films of copper and silver similar to those of Lin and Leonard[23], and Worobey *et al.*[24] on gold would be useful to verify the results of this work.

Low Temperature Results

The original purpose of the low temperature measurements was to determine the size effect on the phonon-drag thermoelectric power. While there are some indications of such an effect in the case of silver and gold (note the hint of a broad negative peak in the thermoelectric power of the thicker foils, where the magnetic impurity effect has not yet grown to total prominence) it was obvious that another, much larger, effect was predominant. Examination of the results in terms of magnetic impurity scattering and size effect has led to some rather surprising results.

The peak height due to iron has given us a value for $\rho_3 S_o$ which is a measure of the unoxydized magnetic impurity present in the sample. As is seen in Eq. (34) our results depend only upon the resistivity of the wire and foil and the absolute temperature. Methods I and II give two approaches for separating S_o and ρ_3. Using published data on the concentration of iron as a function of residual resistivity, we can obtain from ρ_3 an estimate of the concentration of the unoxydized magnetic impurity that is present in the samples. This has exciting possibilities as a tool with which to determine low level iron concentrations in the noble metals.

The study of iron impurities in the noble metals is of great interest. All work to date has been at low temperatures (less than 10 ^{o}K) because above this temperature the effect is masked by other scattering. The size effect experiment, however, effectively cancels out all other effects other than that of the magnetic impurity. Thus, this method provides a means for studying magnetic impurities over the entire temperature range of the effect.

A next step in the development of this technique into a useful and accurate measure of sub-ppm concentrations of iron, would be to carry out a controlled study of a series of wires with known iron concentrations measured against a standard foil size of high purity. The present experiment was not designed to study magnetic impurities, and in fact all efforts were made to prepare samples with values of the resistance ratio (RR) as high and as reproducible as possible. In light of our present analysis this gives a very small spread in impurity concentrations, and thus it would be desirable to perform this experiment with a wider range of resistance ratios and therefore a wider range of impurity concentrations. Also, more detailed information is needed on the constant of proportionality relating residual resistivity and iron concentration for a wide range of dilute alloys (less than 100 ppm). This could be accomplished by making residual resistivity measurements for a series of carefully prepared dilute alloy samples. It would also be helpful to have knowledge of S_o at higher temperatures and a more complete knowledge of T_o for thermoelectric measurements. To our knowledge this is the first experimental method capable of yielding such information.

Representative samples of gold, copper, and silver, both before and after annealing, were analyzed by atomic absorption spectroscopy. In each case no iron, chromium, or manganese was found within the stated accuracy of the instrument, 0.05 ppm.

Sources of Error

The accuracy of temperature measurements is estimated to be better than 0.1 ^{o}K and is limited to that only by heat leaks at large temperature gradients. The control of the temperature is estimated to be 0.0001 ^{o}K at 4.2 ^{o}K and 0.005 ^{o}K at 77.3 ^{o}K. Relative voltage measurements are estimated to be accurate to 0.01 μV. Thus, errors inherent in the measurement of the thermoelectric emf, resistance, errors due to temperature drifts, and other systematic instrument errors are not large enough to have any significant effect on the results of this experiment.

Sources of error that do contribute significantly are those caused by sample preparation, non-uniformity in the thickness of foils, and the presence of holes in the foils due to rolling.

The error indicated in the values of U and V obtained in this experiment represent only the standard deviation resulting from a least squares fit of the data. The error indicated in the results of Lin and Leonard[23] also include measurement errors. It is not known how Huebener[10] and Worobey *et al.*[24] obtained their larger stated error of ±0.19 and ±0.20 respectively. Using Huebener's[10] published data a value of ±0.06, based on the standard deviation, for the error in U and V was calculated.

LIST OF REFERENCES

1. N. F. Mott and H. Jones, "The Theory of the Properties of Metals and Alloys" (Dover Publications, Inc., New York, 1958).

2. A. H. Wilson, "The Theory of Metals" (Cambridge University Press, New York, 1953).

3. D.K.C. MacDonald, "Thermoelectricity: An Introduction to the Principles" (Wiley, New York, 1962).

4. J. M. Ziman, "Electrons and Phonons" (Oxford University Press, Oxford, England, 1960).

5. J. M. Ziman, *Advan. Phys. 10*, 1 (1961).

6. P. L. Taylor, *Proc. Roy. Soc. (London) A275*, 209 (1963).

7. F. J. Blatt, *Phys. Letters 8*, 235 (1964).

8. L. Colquitt, Jr., H. R. Fankhauser, and F. J. Blatt, *Phys. Rev. B4*, 292 (1971).

9. J. E. Robinson, *Phys. Rev. 161*, 533 (1967).

10. R. P. Huebener, *Phys. Rev. 136*, A1740 (1964).

11. E. Justi, M. Kohler, and G. Lautz, *Naturwissenshaften 38*, 475 (1951); *Z. Naturforsch 6a*, 456, 544 (1951).

12. J. Savornin and G. Couchet, *C. R. Acad. Sci. Paris 234*, 1608 (1952).

13. J. Savornin and F. Savornin, *J. Phys. Radium 17*, 283 (1956).

14. F. Savornin, *Ann. Phys. (Paris) 5*, 1355 (1960).

15. F. Savornin, J. Savornin, and A. Donnadieu, *C. R. Acad. Sci. Paris 254*, 3348 (1962).

16. L. Reimer, *Z. Naturforsch 12a*, 525 (1957).

17. R. Nossek, *Z. Naturforsch 16a*, 1162 (1961).

18. R. P. Huebener, *Phys. Rev. 140*, A1834 (1965).

19. J. Gouault, *J. Phys.* *28*, 931 (1967).

20. J. Gouault and M. Hubin, *C. R. Acad. Sci. Paris* *B265*, 1478 (1967).

21. I. Holwech and V. Sollien, *Phys. Stat. Sol.* *34*, 403 (1969).

22. R. K. Angus and I. D. Dalgliesch, *Phys. Letters* *31A*, 280 (1970).

23. S. F. Lin and W. F. Leonard, *J. Appl. Phys.* *42*, 3634 (1971).

24. W. Worobey, P. Lindenfeld, and B. Serin, *Phys. Letters* *16*, 15 (1965); in "Basic Problems in Thin Films" (R. Niedermayer and H. Mayer, eds.), p. 601 (Vandenhoeck and Ruprecht, Göttingen, 1966).

25. *Ibid.*

26. A. V. Gold, D.K.C. MacDonald, W. B. Pearson, and I. M. Templeton, *Phil. Mag.* *5*, 765 (1960).

27. W. B. Pearson and I. M. Templeton, *Can. J. Phys.* *39*, 1084 (1961).

28. D.K.C. MacDonald, W. B. Pearson, and I. M. Templeton, *Proc. Roy. Soc.* *A266*, 161 (1962).

29. C. Van Baarle and F. W. Gorter, *Physica* *32*, 1709 (1966).

30. A. M. Guénault, *Phil. Mag.* *15*, 17 (1967).

31. E. R. Rumbo, *Phil. Mag.* *22*, 953 (1970).

32. J. Kondo, *Progr. Theoret. Phys. (Kyoto)* *32*, 37 (1964).

33. J. Kondo, *Progr. Theoret. Phys. (Kyoto)* *34*, 372 (1965).

34. J. Kondo, *Solid State Phys.* *23*, 184 (1969).

35. E. H. Sondheimer, *Advan. Phys.* *1*, 1 (1952).

36. J. S. Dugdale and M. Bailyn, *Phys. Rev.* *157*, 485 (1967).

37. P. E. Nielson and P. L. Taylor, *Phys. Rev. Letters* *21*, 893 (1968).

38. P. E. Nielson and P. L. Taylor, *Phys. Rev. Letters* *25*, 371 (1970).

39. P. E. Nielson and P. L. Taylor, A.E.C. Technical Report No. 65, C00-623-152, unpublished (1970).

40. R. R. Bourassa and A. W. Dudenhoeffer, *Phys. Rev.* *B7*, 1270 (1973).

41. A. W. Dudenhoeffer and R. R. Bourassa, *Phys. Rev.* *B5*, 1651 (1972).

42. R. P. Huebener, *Phys. Rev. 135*, A1281 (1964).

43. J. Kondo, *Solid State Phys. 23*, 184 (1969).

44. L. Nordheim and C. J. Gorter, *Physica 2*, 383 (1935).

45. M. Bailyn, *Phil. Mag. 5*, 1059 (1960).

46. M. Bailyn, *Phys. Rev. 120*, 381 (1960).

47. P. G. Klemens, *Solid State Physics 7*, 1 (1958).

48. A. M. Guénault, *Phil. Mag. 133*, 17 (1967).

49. C. Van Baarle, *Physica 33*, 424 (1967).

50. C. Van Baarle and R. P. Huebener, *Phys. Letters 23*, 189 (1966).

51. M. Bailyn, *Phys. Rev. 157*, 480 (1967).

52. F. R. Fickett, "Oxygen Annealing of Copper: A Preliminary Review", Cryogenics Division, National Bureau of Standards, Institute for Basic Standards, Boulder, Colorado 80302 (to be published).

53. A. C. Ehrlich, "Oxygen Annealing of Silver for Obtaining Low-Electrical Resistivity: Technique and Interpretation", Naval Research Laboratory, Washington, D. C. 20375 (to be published).

54. R. P. Ries and B. K. Moore, *Rev. Sci. Instr. 41*, 996 (1970).

55. W. B. Pearson, *Can. J. Phys. 38*, 1048 (1960).

56. M. D. Daybell and W. A. Steyert, *Rev. Mod. Phys. 40*, 380 (1968).

57. G. K. White and S. B. Woods, *Can. J. Phys. 33*, 58 (1955).